Anomalies, Artifacts and Common Errors in Using Vibrational Spectroscopy Techniques

Mid-infrared Spectroscopy: Anomalies, Artifacts and Common Errors

John M. Chalmers
University of Nottingham, Nottingham, UK

1 INTRODUCTION

Anomaly ("irregularity, deviation from rule"),[1] artifact/artefact ("a thing made by human workmanship"),[1] and error ("deviation from the right way, blunder, mistake, wrong-doing"):[1] three nouns (and their dictionary definitions) that when applied to an infrared (IR) (or indeed any vibrational) spectrum or spectral feature immediately imply that the data are imperfect, that the data were derived in an imperfect way, or that the data are impure. There are many sources that give rise to such observations and comment. Many are derived from poor experimental practice (e.g. poor grinding of the analyte in an alkali-halide disk preparation), some from inappropriate sampling, some from contamination (e.g. silicone grease from vacuum apparatus), others from instrumental limitations (e.g. too low an angle of incidence in an attenuated total reflection (ATR) measurement), some from the environment (e.g. intrusion of absorptions due to atmospheric water vapor and carbon dioxide), while others classified similarly merely reflect the fact that the measurement was made at an extreme (e.g. photoacoustic saturation). Some may merely be a nuisance and not detract from the measurement purpose, while others are disastrous and can lead to erroneous conclusions.

Understanding, appreciating and recognizing anomalies, artifacts and common errors is vital if data are to be interpreted and quantified correctly. The intention in this article is to present examples of common imperfections observed in mid-infrared spectra and to discuss concisely their origin, utilizing, wherever possible, example spectra to highlight issues. It cannot hope to cover all such occurrences, but will hopefully instil precaution and caution in experimentalists and researchers new to the technique.

2 ATMOSPHERIC INTRUSION

Perhaps the most readily recognized imperfections in any IR spectrum, whether, for example, it is a transmission, emission, or photoacoustic measurement, are those absorption bands arising from the presence of atmospheric molecules in the path of the IR beam between the source and the detector. (This, of course, excludes circumstances where they are required for detection or calibration.) A ro-vibrational mid-infrared transmission spectrum depicting these features is shown in Figure 1. It comprises absorption bands due to both water vapor and carbon dioxide. Their spectral contrast and relative intensity will depend on the spectral resolution of the measurement, the relative concentration of the two gases, and, in some experiments, perhaps their partial pressure and temperature. (Including this imperfection may seem overly trivial to experienced spectroscopists; however, I have seen changes in the relative intensity of the CO_2 bands near $2350\,cm^{-1}$ reported in a conference proceedings abstract as being indicative of a change in the level of cure in a polymer composite!) These bands due to water vapor and carbon dioxide when seen in a Fourier transform infrared (FT-IR) spectrum may be observed as either with positive or negative intensity, depending on the relative extents to which they were present in the sample and background single-beam spectra of an FT-IR spectrum measurement.

Since, there is no change of dipole moment associated with the stretching frequencies of homonuclear diatomics, then neither nitrogen nor oxygen give rise to IR absorption

Handbook of Vibrational Spectroscopy, Online © 2006 John Wiley & Sons, Ltd.

This article was published in the *Handbook of Vibrational Spectroscopy* in 2006 by John Wiley & Sons, Ltd.
DOI: 10.1002/9780470027325.s3101

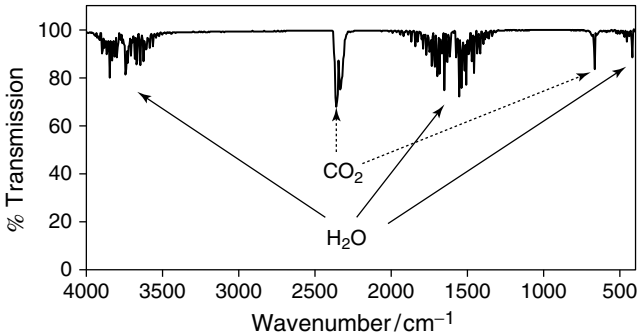

Figure 1. IR transmission spectrum showing absorption bands characteristic of atmospheric water vapor and carbon dioxide. The 4 cm^{-1} resolution spectrum was generated by ratioing FT-IR open single-beam spectra recorded with the sample compartment of the spectrometer unpurged against that with the compartment purged with dry nitrogen.

bands. Their presence, along with other environmental phenomena, such as cosmic rays or lamp emissions, may however be sometimes detected within Raman spectra (see **Anomalies and Artifacts in Raman Spectroscopy**).

3 SUPERIMPOSITION OF A SINUSOIDAL WAVEFORM

The appearance of a sinusoidal waveform overlaying an IR spectrum is yet another common cause of imperfection that is generally well recognized, and is usually most noticeable in baseline regions, where there are no absorption bands. The frequency and amplitude of the sinusoidal wave will depend on its origin, and its intrusiveness may depend also on the spectral resolution. Under some circumstances, the amplitude may change with wavenumber most likely increasing with decreasing wavenumber (increasing wavelength).

Common nomenclatures for such a spectral feature are *interference fringes*, *channel fringes/fringing*, and *channel spectra* (see Glossary to the Handbook). The name used often reflects the favorite of a particular community. For example, the term "interference fringes" is most commonly used to describe the effect when observed in thin film polymer spectra, where they originate as a consequence of the sample being thin, non-scattering and of uniform thickness. "Channel spectra" is the frequently used descriptor for their appearance in high-resolution gas-phase spectra, where they are instrument related, arising from parallelism within an interferometer beam-splitter/compensator assembly. Whatever their source, they arise from an interference pattern generated between the recombination of two coherent IR beams that have travelled a different pathlength.

The effect is perhaps most easily illustrated in the practice of determining the pathlength of an empty IR transmission cell, as shown in Figure 2. When the optical path difference between the two beams equals $\lambda/2$ then destructive interference will occur, where λ represents the wavelength. At optical path differences equal to integral multiples of a wavelength, then the two beams will be in phase and constructive interference will occur, i.e. their intensities will be additive. The fringe separation, frequency of the waveform, for two differing pathlengths is also shown in Figure 2. Figure 3 illustrates the waveform that might be observed from a slightly wedged source for the interference pattern. Figure 4 shows two examples of *fringing* observed in IR transmission spectra recorded from thin polymer films.

4 STRAY LIGHT

For stray light, the Glossary to this Handbook contains the two definitions following: "Radiation that does not follow

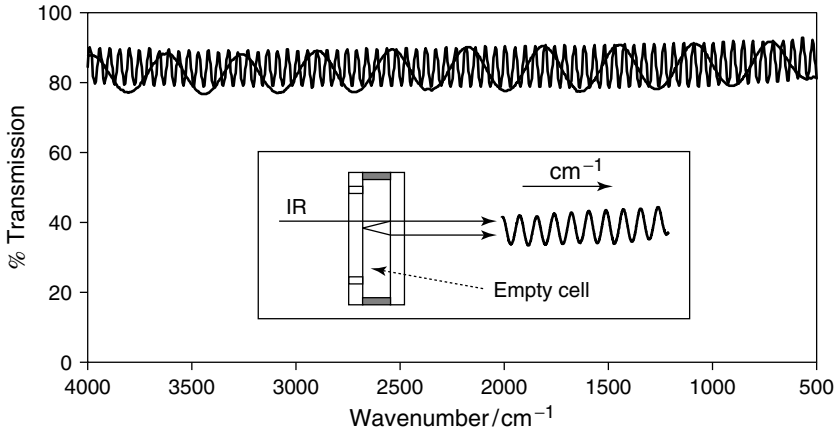

Figure 2. Overlaid 4 cm^{-1} resolution, transmission IR spectra recorded from empty (air gap) transmission IR liquid cells. The pathlengths of the air gaps were: 12.5 μm, low-frequency sinusoidal wave; 100 μm, high-frequency sinusoidal wave. A schematic of the process producing interference fringes in the IR spectrum recorded from a thin, empty transmission liquid cell is shown in the inset.

Handbook of Vibrational Spectroscopy, Online © 2006 John Wiley & Sons, Ltd.

This article was published in the *Handbook of Vibrational Spectroscopy* in 2006 by John Wiley & Sons, Ltd.
DOI: 10.1002/9780470027325.s3101

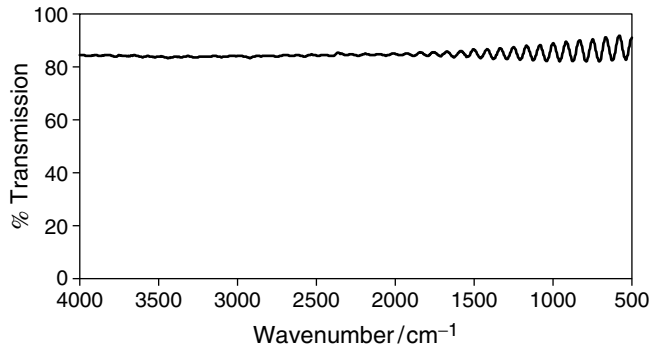

Figure 3. Transmission spectrum recorded from an empty wedged nominal 50 µm pathlength liquid cell. Loosening the retaining screws at one end of the cell assembly produced the non-parallelism of the cavity.

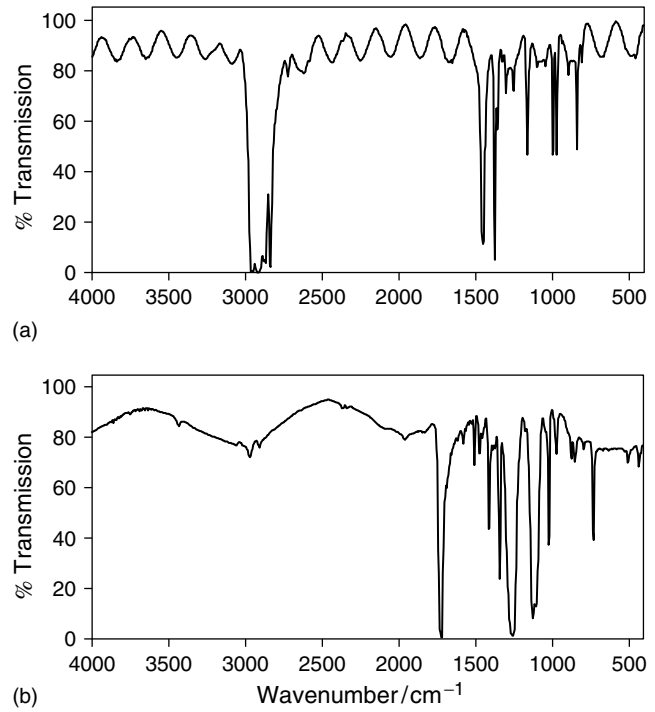

Figure 4. Transmission IR spectra, 4 cm^{-1} resolution, showing interference fringes recorded from polymer films: (a) 20 µm thickness polypropylene; (b) 2.5 µm thickness poly(ethylene terephthalate) (PET).

the usual path through a spectrometer and consequently appears in a spectrum at a wavenumber different from its true wavenumber. The term is also used to refer to radiation that passes around the sample instead of through it, and consequently is not modified by the sample and seriously affects absolute and relative intensities." In this section, we will be considering the second classification for the measurement error. It will be broadened, however, to include a discussion of examples where the radiation has passed through the sample, but the sample was not continuous. The straylight phenomenon in this case arises from the likes of a bubble in a liquid in a cell or a polymer film in a transmission measurement.

IR radiation that has travelled the conventional path and reached the detector without having passed through the sample will adversely affect the spectral contrast of any measurement. It will probably have serious deleterious consequences on any quantitative determinations made from the spectrum. It causes loss of spectral contrast, and can affect bands of differing absorptivities to different extents. Unhindered stray light, that is radiation that bypasses the sample and effectively passes straight from the source to the detector, will shift the zero position of the transmission scale on the measured spectrum.

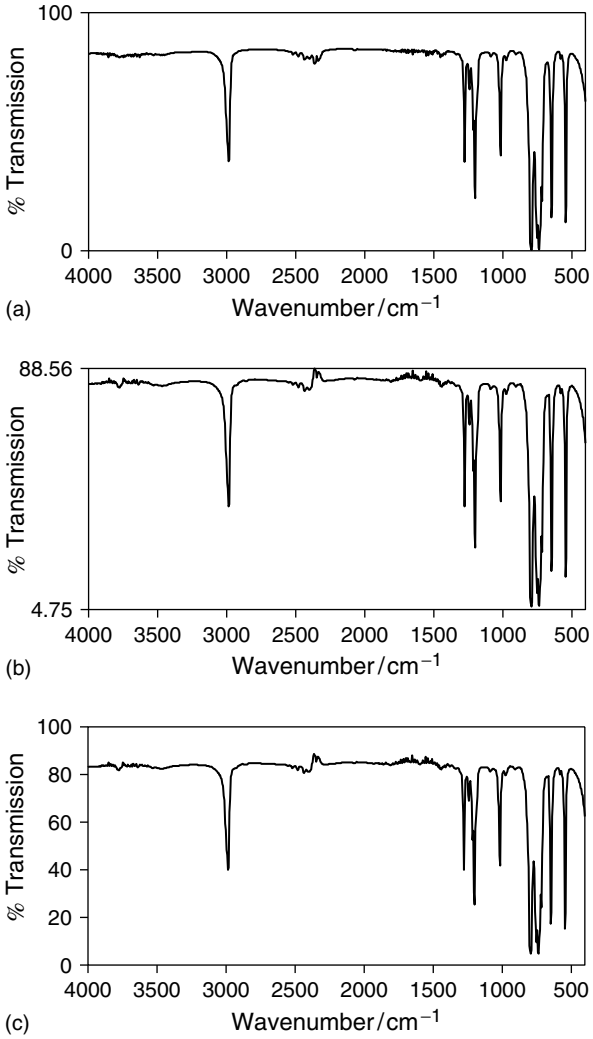

Figure 5. IR transmission spectra, 4 cm^{-1} resolution, recorded from 1,1,2,2-tetrachloroethane in a 12 µm pathlength liquid cell. The spectrum plotted as full ordinate scale expansion shown as (b) was recorded from a specimen that had a few small bubbles in it; the liquid completely filled the cell cavity when the spectrum shown as (a) was recorded. The spectrum shown as (c) is from the same recording as for (b) but plotted on an ordinate scale of 100–0% transmission.

Handbook of Vibrational Spectroscopy, Online © 2006 John Wiley & Sons, Ltd.

This article was published in the *Handbook of Vibrational Spectroscopy* in 2006 by John Wiley & Sons, Ltd.
DOI: 10.1002/9780470027325.s3101

Figure 5 shows two transmission spectra recorded from the solvent 1,1,2,2-tetrachloroethane contained in a 12-μm pathlength IR transmission cell. Neglecting the differences as a consequence of differing contributions from atmospheric water vapor and carbon dioxide, these two spectra look essentially identical, and each could readily be used to characterize the solvent. The lower spectrum was output to a recorder using an automated software command that set the minimum and maximum transmission values to full scale. This is not an uncommon practice. The ordinate values of Figure 5(a) extend from 100 to 0% transmission, while those of Figure 5(b) only extend from 88.56 to 4.75% transmission. While the maximum value is of no significant consequence here, the minimum is! The spectrum of Figure 5(b) was generated from a sample that had a few small bubbles in it, that is the solvent did not fully fill the capillary space between the windows of the transmission cell, such that some stray light fell onto the detector. Figure 5(c) shows the spectrum of the sample used to generate the spectrum of Figure 5(b), but this time with the ordinate presented as a full transmission scale. The shift in the true zero is now clearly apparent, and the disastrous consequences on relative band intensities become readily observed in Figure 6, where the absorbance ordinate scale equivalents of Figure 5(a) and 5(b) are compared. A similar *catastrophe* is shown in Figure 7(a) and 7(b), from a pair of transmission spectra generated from the same solvent, but this time the sample was prepared simply as a capillary layer between two KBr windows. The difference between these two consecutively recorded spectra, for example see Figure 7(c), was again a consequence of stray light, but this time the hole was caused by solvent evaporation that occurred between the recording of the two spectra.

The spectra shown in Figure 8 both have ordinate scales that extend down to a transmission value of 0% T. Both

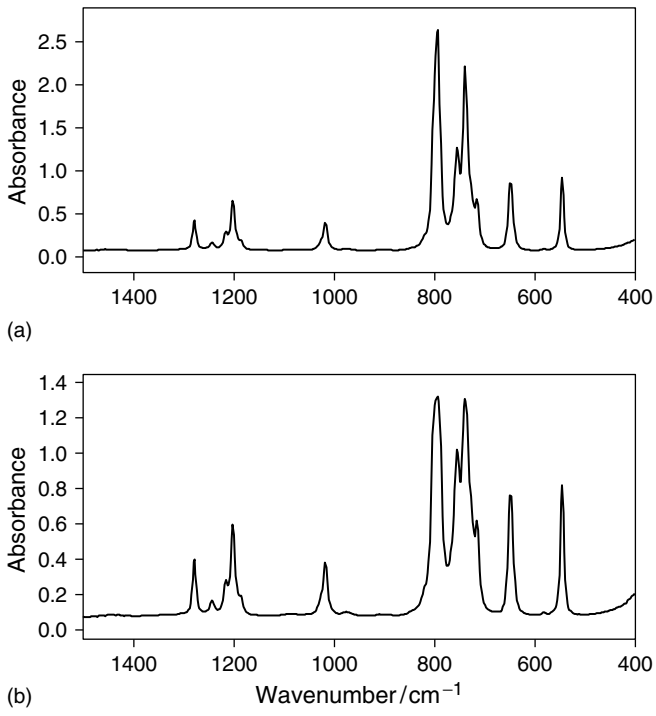

Figure 6. The IR spectra shown as Figure 5(a) and 5(c) but plotted as absorbance spectra over the range 1500–400 cm^{-1} as (a) and (b), respectively.

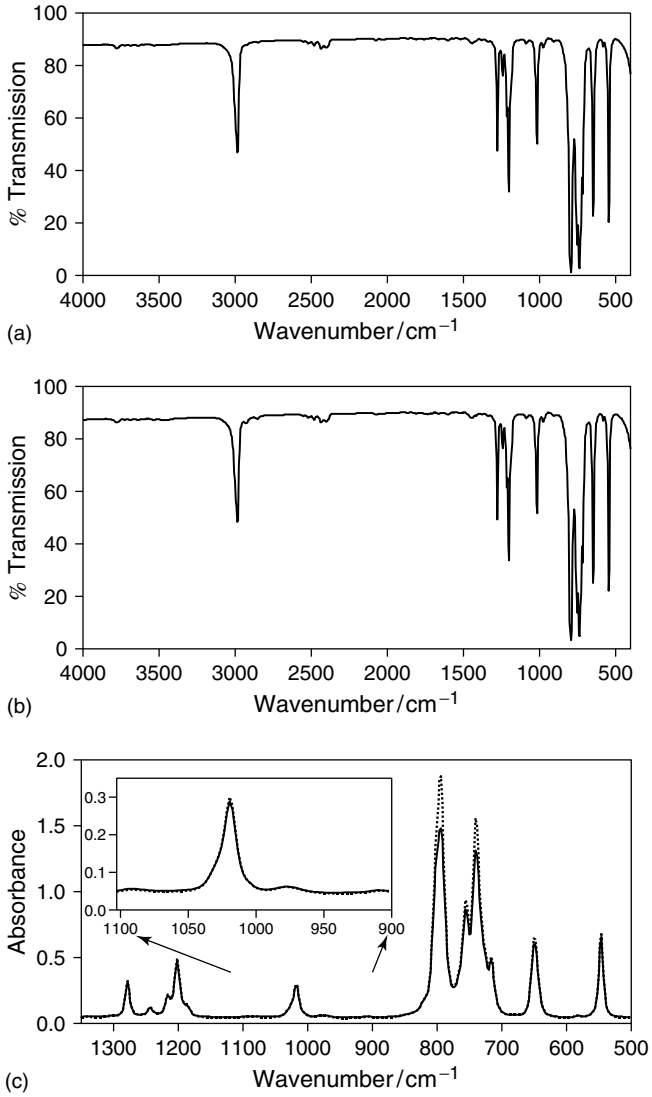

Figure 7. Consecutive IR transmission spectra, 4 cm^{-1} resolution, recorded from 1,1,2,2-tetrachloroethane as a capillary layer between two IR-transparent plates. The second spectrum (b), recorded 5 min after that shown as (a), was recorded from the specimen from which some of the liquid had evaporated, while in the IR beam, leaving a hole (air gap) in the specimen. (c) An overlay of the two spectra in absorbance over the range 1350–500 cm^{-1}. The inset shows the near identical intensities of the band near 1025 cm^{-1}, while the wider range plot shows the large intensity differences between the stronger bands. The dashed line spectrum is equivalent to (a), and the solid line corresponds to (b).

Handbook of Vibrational Spectroscopy, Online © 2006 John Wiley & Sons, Ltd.

This article was published in the *Handbook of Vibrational Spectroscopy* in 2006 by John Wiley & Sons, Ltd.
DOI: 10.1002/9780470027325.s3101

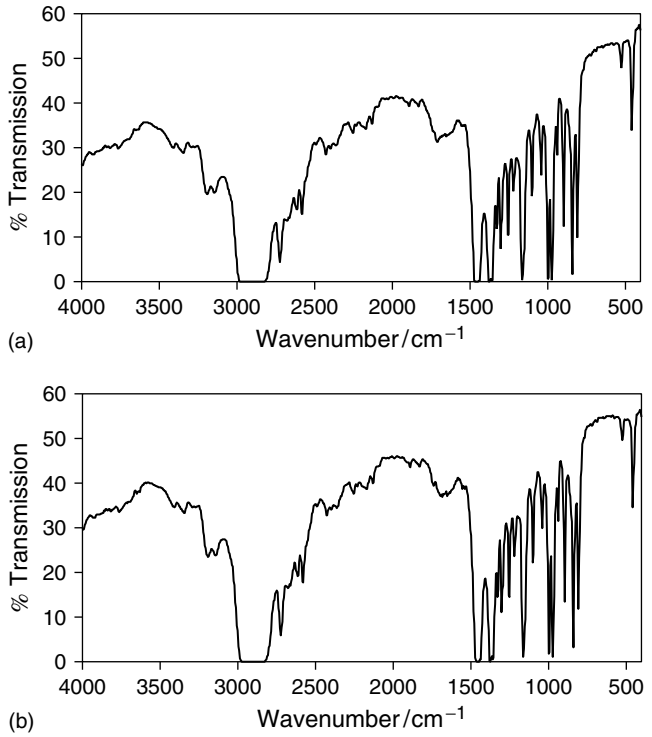

Figure 8. IR transmission spectra, 4 cm^{-1} resolution, recorded from two compression molded film samples of polypropylene. Spectrum (a) was recorded from a specimen without bubbles, whereas (b) was recorded from a specimen containing a few small bubbles. See text for more details.

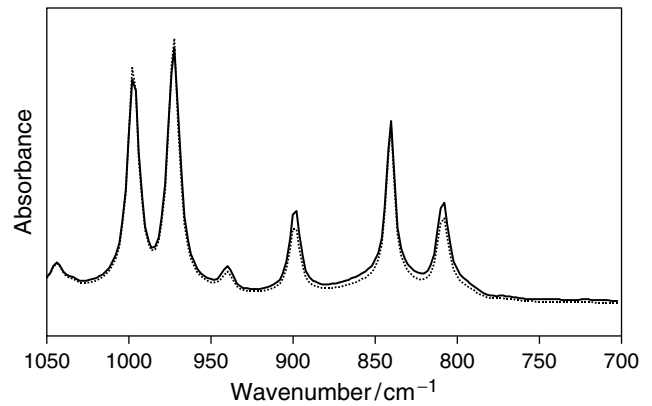

Figure 9. Overlaid absorbance spectra over the range 1050–700 cm^{-1} generated from the two transmission spectra shown in Figure 8. The dashed line is for the continuous film, and the solid line is for the film that contained bubbles.

were recorded from samples of a polypropylene film, each of a thickness of about 0.15 mm, and both serve as excellent *fingerprint* spectra of the material. The spectrum of Figure 8(b) extends to 0% T, since the thickness of polypropylene through which the IR radiation passed was such that it provided extinction for bands with high absorptivities. However, while no IR radiation bypassed the sample, it was recorded from a sample that contained a few small bubbles that were generated by molding the film sample at too high a temperature. The sample used for Figure 8(a) prepared under optimal molding conditions was continuous and contained no visual bubbles. The deleterious consequence for quantitative measurements from such a non-continuous sample is illustrated in the comparison of the two spectra made in Figure 9. While undoubtedly some of the differences in relative band intensities between the spectra occur as a result of the differing thermal histories of the two specimens, the bubbles in the film sample are also responsible for some of the variation.

5 CONTAMINATION

To many readers, contamination may seem too obvious a form of spectrum impurity to include as a section in this article, but sources that are obvious to many are still novel to some, and indeed have been overlooked in research publications by experts (although no references will be quoted for these!). In the context here, "contamination" refers to materials that give rise to absorption bands that may be misinterpreted as being attributable to the sample in its expected form. The examples here cannot be exhaustive; they will vary widely among different application areas. The three selected as illustrations are from my experience and encounters. They will hopefully help instil a discipline of looking at a spectrum initially with some lateral interrogation as opposed to solely focusing on the *problem in hand* or anticipated/predicted result (as clearly happened with the publications alluded to above).

Residual solvent in a sample cast from solution is an obvious source of spectral impurity, and attributed absorption bands are usually readily observable. However, some samples may deposit in a form that contains the solvent as "solvent of crystallization". For more on this and similar spectral manifestations, the reader is referred to the article on polymorphism in Volume 5 of this handbook (**Polymorphs, Solvates and Hydrates**).

After a few preparations, most experimentalists have grown accustomed to the improbability of ever making a KBr disk preparation that is entirely free from absorbed water and observing the consequent broad absorption νOH at ca. 3400 cm^{-1} and maybe the δHOH band near 1640 cm^{-1}. However, to the unknowing there is potentially a nastier danger lurking in commercial supplies of the alkali halide. This lies in contamination by the nitrate ion, NO_3^-. Unless one purchases "spectroscopic grade" KBr, one is very likely to find the material contaminated with low levels of KNO_3. NO_3^- gives rise to a narrow band with very high absorptivity near 1380 cm^{-1}; it may be confused, for instance, with the deformation mode of a $-CH_3$ group that might be present in the analyte of a KBr disk preparation.

Handbook of Vibrational Spectroscopy, Online © 2006 John Wiley & Sons, Ltd.

This article was published in the *Handbook of Vibrational Spectroscopy* in 2006 by John Wiley & Sons, Ltd.
DOI: 10.1002/9780470027325.s3101

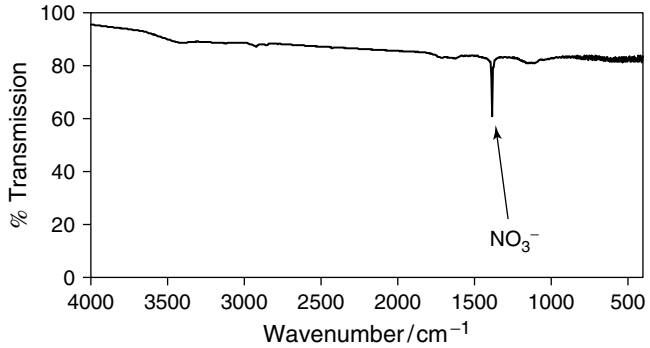

Figure 10. IR transmission spectrum of a KBr disk preparation made using "non-spectroscopic grade" KBr; the absorbance peak near 1380 cm^{-1} due to nitrate is clearly evident. The background spectrum for this FT-IR measurement was made using spectroscopic-grade KBr. (Some interference fringes from the disk are evident too, more strongly towards lower wavenumber. Other weak absorption bands are associated with the analyte being examined.)

The spectrum shown in Figure 10 was generated recently (while this handbook was in preparation) as a consequence of an attempt by a laboratory technician in an academic institution to find an alternative supply of KBr in a teaching laboratory.

Silicone oil and silicone grease in the form of poly(dimethyl siloxane) (PDMS) are potentially major sources of contamination, and anyone not involved directly in characterizing silicone materials should be very suspicious of any spectrum that has a sharp band at 1260 cm^{-1}. It is a distinctive feature of PDMS, and its presence or otherwise may be ascertained by reference to its other characteristic absorption features shown in Figure 11. PDMS is potentially a common source of contamination for those using vacuum apparatus and desiccators. I have seen bands of PDMS assigned to other species in both a PhD thesis and a research publication in a highly respected spectroscopic journal. In a similar context, "phthalate plasticizer" (a di-alkyl phthalate) is a common source of

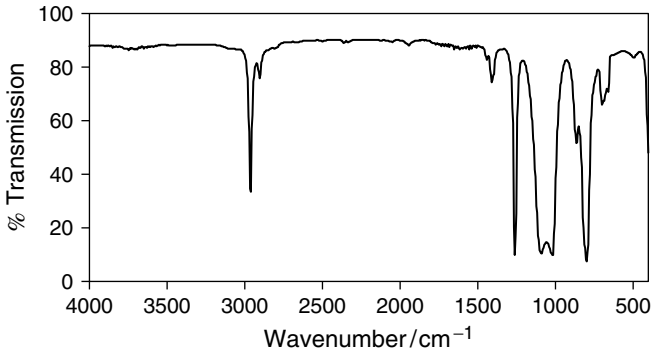

Figure 11. IR, 4 cm^{-1} resolution, transmission spectrum recorded from a capillary layer of silicone vacuum grease. The spectrum is that of PDMS.

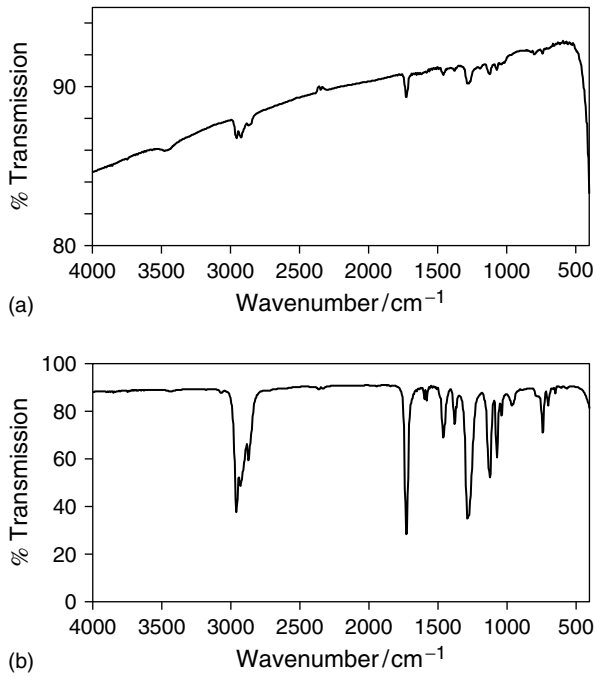

Figure 12. IR, 4 cm^{-1} resolution, transmission spectra recorded from: (a) a deposit on a KBr plate generated by touching one surface of the plate with a finger while wearing PVC gloves that were slightly wet with chloroform; (b) a reference sample of a phthalate plasticizer.

invasive contamination from poly(vinyl chloride) (PVC) products, such as PVC piping and protective PVC gloves (see Figure 12(a)). An example of a phthalate plasticizer spectrum is shown in Figure 12(b), the νC=O at about 1725 cm^{-1} and accompanying weak sharp doublet near 1600 cm^{-1} are usually the give-away features.

6 ANOMALOUS DISPERSION

A key intrinsic property of a sample to mid-infrared measurements, particularly those made by a reflection technique, is its refractive index. The refractive index, n, and absorption index, k, are interrelated through the Fresnel laws of reflection and the Kramers–Kronig (K–K) relationship; see, for example, **External Reflection Spectroscopy** by Claybourn in this handbook. As one scans through an absorption band, then the refractive index of the sample changes from the average value at positions either side of the band, where the sample does not absorb IR radiation. For organic materials, this change is usually observed as a lowering of the sample refractive index to the high-wavenumber side of the absorption band maximum, returning to the average value at the absorption band center, then increasing to the lower-wavenumber side, before returning again to the average value. This is known as *anomalous dispersion* and is illustrated in Figure 13. This dispersion in a

Handbook of Vibrational Spectroscopy, Online © 2006 John Wiley & Sons, Ltd.

This article was published in the *Handbook of Vibrational Spectroscopy* in 2006 by John Wiley & Sons, Ltd.
DOI: 10.1002/9780470027325.s3101

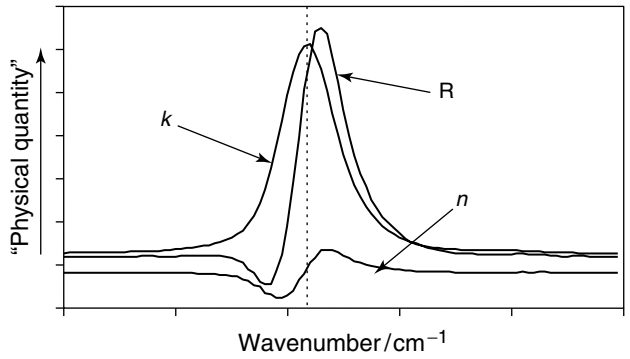

Figure 13. Representative spectra superimposed of reflectance, R, absorption index, k, and refractive index, n.

sample's refractive index, which increases with increasing absorptivity, can feature in many reflection measurements of mid-infrared spectra, and as a consequence it is important that its effect is fully appreciated.

An important consequence of anomalous dispersion is the Christiansen effect that may be observed readily in the spectrum recorded from a non-optimal specimen preparation of a powder sample as a mull or an alkali-halide disk (see next section). As examples in this section, we will discuss mid-infrared measurements made by the transflection and internal reflection spectroscopy techniques.

In a transflection experiment, the measurement is usually made from a thin (typically 0.5 to a few micrometers thickness, t) continuous, non-scattering sample, often a polymer film, deposited on a non-IR absorbing reflective substrate, such as a polished metal surface. The radiation is incident on the sample at near normal (low angles) of incidence, θ, and the detected radiation is a composite of radiation that has been specularly reflected from the front surface and that which has passed through the sample and been reflected from the reflective substrate. The latter contribution is usually dominant, and the recorded spectrum resembles closely that of a transmission spectrum of a thickness equivalent to $2t/\cos\theta'$, where θ' represents the angle of refraction within the sample layer. However, in regions of high absorptivity, that is for strongly absorbing bands, then the specular component may become pronounced, particularly if the sample thickness is low. Figure 14 shows a transflection spectrum recorded directly from a non-stick coating on a baking tray. The significant effects, that is of apparent band multiplicity and inversion, on the stronger absorption bands is clearly evident, when this spectrum is compared with the reflection and absorption index spectra in the lower part of Figure 14. These spectra, for comparison, were a pure front-surface reflection spectrum recorded from a thick sample of polymer similar to that used for coating the baking tray and the absorption index spectrum generated via the K–K transform of this front-surface reflection spectrum.

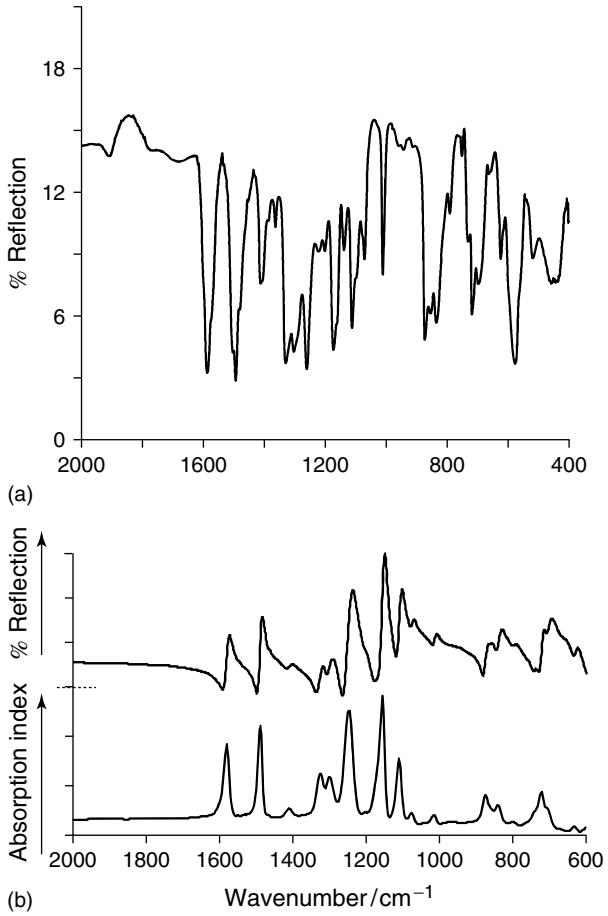

Figure 14. (a) Transflection IR spectrum recorded from a PES coating on a baking tray. (b) Reflection IR spectrum recorded from the surface of a thick molding of PES, and the subsequently derived K–K algorithm absorption index spectrum.

(The polymer being examined was a poly(aryl ether sulfone), PES.)

More subtle imperfections may be observed in some spectra that are recorded using the internal reflection technique. As an example, two spectra recorded from the surface of a polyester film are shown in Figure 15. The spectra appear to differ slightly. The internal reflection spectrum shown as Figure 15(a) was recorded using a parallelipiped KRS-5 prism with an incidence angle of 60°; the internal reflection spectrum shown as Figure 15(b) was again recorded using a parallelipiped KRS-5 prism, but this time using an incidence angle of 45°. Some of the differences in relative band intensities might be accounted for by gradients or anisotropy in surface-layer morphology because of the differing surface layer thickness sampled in these two measurements. However, in the context of anomalous dispersion, one should note in particular, for example, the increased asymmetry to the lower wavenumber side of the absorption bands at about 1725 cm^{-1} and 1250 cm^{-1} in Figure 15(b) compared with those in Figure 15(a). These

Handbook of Vibrational Spectroscopy, Online © 2006 John Wiley & Sons, Ltd.

This article was published in the *Handbook of Vibrational Spectroscopy* in 2006 by John Wiley & Sons, Ltd.
DOI: 10.1002/9780470027325.s3101

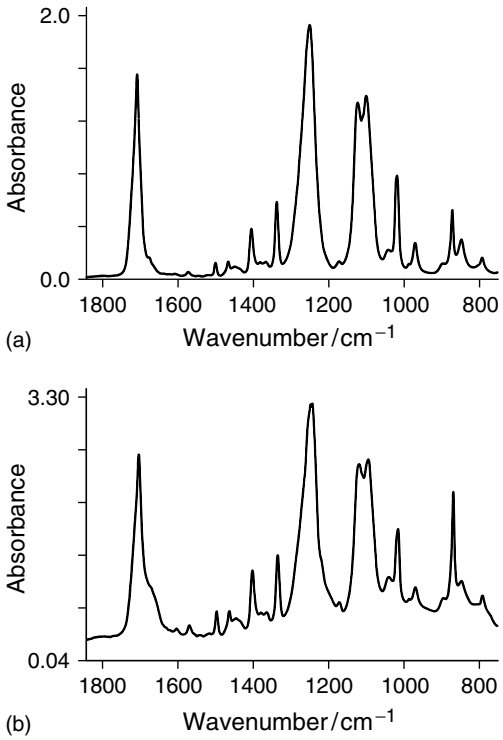

Figure 15. IR internal reflection spectra, 4 cm^{-1} resolution, plot as absorbance spectra recorded using KRS-5 parallelepiped reflection elements with both sides covered with PET film. The multiple internal reflection elements were: (a) a 50 mm × 3 mm element with an incidence angle of 60°; (b) a 30 mm × 3 mm element with an incidence angle of 45°.

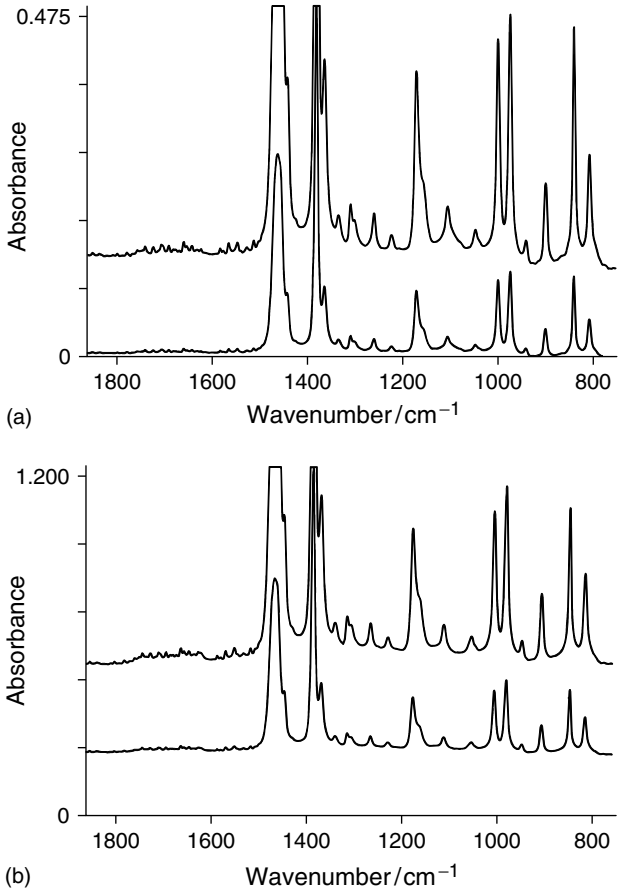

Figure 16. IR internal reflection spectra, 4 cm^{-1} resolution, plot as absorbance spectra recorded using KRS-5 parallelepiped reflection elements with both sides covered with polypropylene film. The multiple internal reflection elements were: (a) a 50 mm × 3 mm element with an incidence angle of 60°; (b) a 30 mm × 3 mm element with an incidence angle of 45°. The upper plot on each has been scale expanded.

are artifacts, which might be misinterpreted; for instance, one might have assigned the perceived shoulder at about 1700 cm^{-1} in Figure 15(b) to potentially indicate a high level of surface carboxylate end groups, since the film being examined was PET. (However, intuitively, if this were true then the concentration would be greater in the spectrum of Figure 15a, where a shallower surface layer is probed.) These *artifacts* arise from the fact that around the positions of the maxima of these bands with high absorptivities, then the condition for ATR becomes violated. That is, since the angle of incidence at these positions is no longer greater than the critical angle, then external rather than total internal reflection occurs at the internal reflection element/sample boundary. (The critical angle, θ_c, is given by $\sin\theta_c = n_2/n_1$, where n_1 is the refractive index of the internal reflection element, in this case KRS-5 with $n_1 = 2.37$, and n_2 is the refractive index of the sample. If we assume $n_2 = 1.5$ for the sample in regions where it does not absorb, then $\theta_c \approx 39°$. If n_2 rises to ca. 1.705, then θ_c becomes about 46°, that is, it is now above the angle of incidence used to record the spectrum shown as Figure 15b.) For a similar comparison on a sample with bands of generally lower absorptivities, that is a polypropylene film, then no such gross distortions are observed (see Figure 16(a) and (b)). Figure 17 shows the progression that is also wavenumber dependent, with changing incidence angle from ATR through to external reflection for a nylon film.

Figure 18 shows a diffuse reflection spectrum recorded from powdered PES on the surface of SiC paper after it has been abraded from the surface of a PES molding. Again, overlay of specular reflection can be seen, particularly on the stronger bands, but in this case it is not as severe as for the spectrum recorded in transflection from the baking tray shown in Figure 14.

As a final example in this section, Figure 19 shows FT-IR ATR microscopy spectra recorded from three poly(aryl ether ether ketone) (PEEK) fibers of differing morphologies. The series comprised a non-oriented, low-crystallinity fiber, a uniaxially oriented, low-crystallinity fiber and a uniaxially drawn, crystalline fiber. Although differences associated with increasing crystallinity are clearly

Handbook of Vibrational Spectroscopy, Online © 2006 John Wiley & Sons, Ltd.

This article was published in the *Handbook of Vibrational Spectroscopy* in 2006 by John Wiley & Sons, Ltd.
DOI: 10.1002/9780470027325.s3101

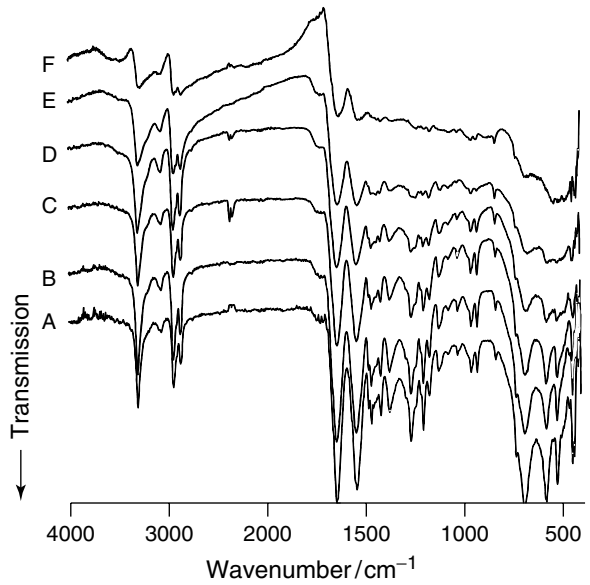

Figure 17. IR internal reflection spectra, 4 cm^{-1} resolution, recorded using a KRS-5 parallelepiped reflection element with both sides covered with a nylon film. The multiple internal reflection element was 50 mm × 3 mm. The assembly was sited in a variable incidence angle accessory, and the spectra were recorded with the accessory set to the following angles: A, 55°; B, 50°; C, 45°; D, 40°; E, 35°; F, 30°. The spectra have been offset for clarity.

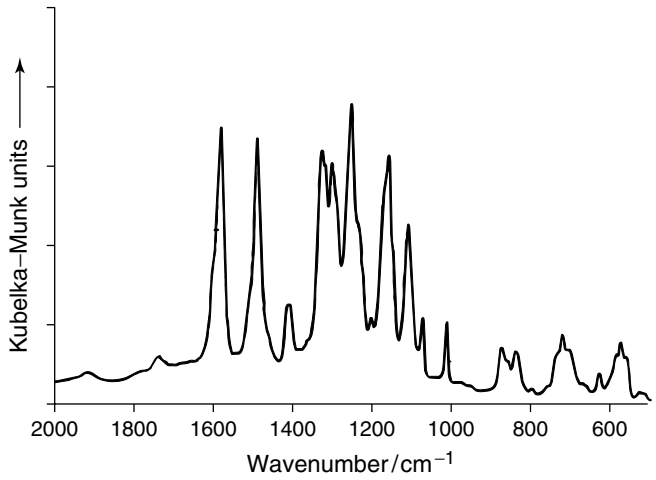

Figure 18. Kubelka–Munk plot from diffuse reflection IR spectrum recorded directly from PES powder abraded from PES molding onto SiC abrasive paper.

shown in, for example, the narrowing of the νC=O ca. 1653 cm^{-1} and the relative intensity ratios of pairs of bands 1305 cm^{-1}/1280 cm^{-1} and 966 cm^{-1}/952 cm^{-1}, the spectra are not pure in terms of their absorbance characteristics. The strong features show distortion, both in terms of their relative intensity and symmetry, when compared with the absorption index spectrum shown for comparison. These spectra are clearly not fit for their intended purpose, which

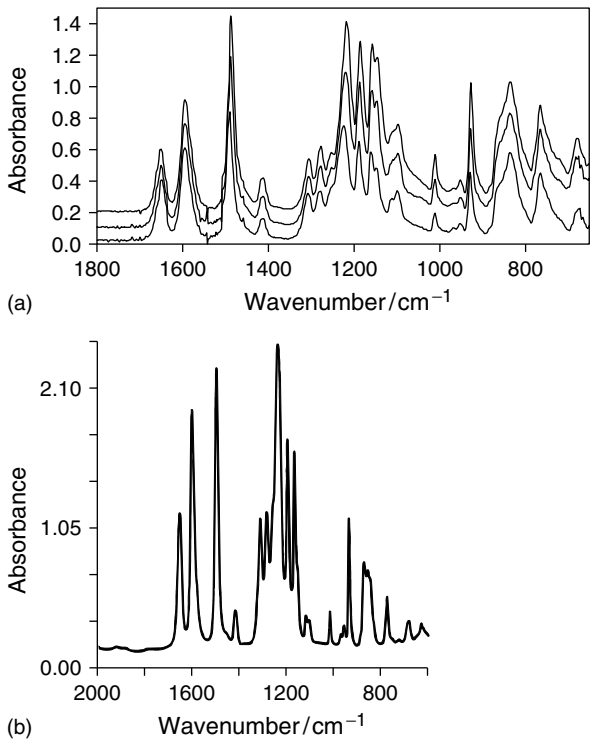

Figure 19. (a) FT-IR ATR microscopy spectra recorded using an objective fitted with a ZnSe ATR element from three samples of PEEK fibers. The upper spectrum is from a non-oriented, low-crystallinity fiber; the middle spectrum is from a uniaxially oriented, low-crystallinity fiber; and the lower spectrum is from a uniaxially drawn, crystalline fiber. The spectra have been offset for clarity. (b) An absorbance spectrum from a thin PEEK film, shown for reference.

was to investigate the possibility of separating (maybe using multivariate analysis techniques) the contributions that might be attributed each to crystallinity and molecular orientation. In an FT-IR ATR microscopy objective, the angle of incidence is usually fixed at a nominal 45°, so this parameter cannot be increased to improve the spectral purity. The ATR element used in this case was of ZnSe, so there is an option of using a higher refractive index element, such as one of Ge, to improve spectral integrity. (These measurements were actually undertaken when commercial ATR objectives were newly being released, and Ge element objectives were not readily available at that time.)

7 PARTICLE SIZE

Mean particle size and particle size distributions are key parameters that greatly affect the appearance of mid-infrared spectra recorded from powders or powder-like specimens, both in terms of spectral contrast and in some cases their background. The theory and much discussion on these parameters appear in the specialist articles on diffuse

Handbook of Vibrational Spectroscopy, Online © 2006 John Wiley & Sons, Ltd.

This article was published in the *Handbook of Vibrational Spectroscopy* in 2006 by John Wiley & Sons, Ltd.
DOI: 10.1002/9780470027325.s3101

reflection in this handbook. The discussion here will be merely concerned essentially with some illustrations of the effects, many extremes, with particle size and packing may have on mid-infrared spectra.

In any mid-infrared measurement from a powder for which the purpose is to obtain a high-quality, good spectral contrast, fingerprint absorption spectrum of a sample, with minimal overlay of *artifact/anomalous* effects, then its mean particle size should be below that of the wavelengths used to interrogate the sample. That is, the largest size of any particle should be less than 10 μm, and preferably below 2 μm.

In transmission measurements made using, for example, an organic powder dispersed in a mulling oil or a KBr disk, then two deleterious effects can be observed if the powder is not finely ground. The first is that of a sloping baseline that decreases towards longer wavelength (lower wavenumber). The second is that referred to as the Christiansen effect, which is imposed as a consequence of asymmetrical scattering loss arising from the dispersion in the refractive index of the sample in the vicinity of its absorption bands. This manifests as a transmission increase on the high-wavenumber side of an absorption band, and a concomitant decrease to the lower-wavenumber side. Both effects can be seen clearly in the mull dispersion spectrum that is shown in Figure 20(a), as can the improvements gained with better grinding of the sample in the spectrum shown in Figure 20(b). The effects are seen more dramatically in the comparison of the KBr disk spectra of Figure 21. Poor dispersion of a coarse powdered analyte in the matrix material adds a third detriment to the recorded spectrum. That is an effect of stray light, since some of the IR radiation may pass through the KBr disk without interacting with the analyte. This effect may well account for the some of the very poor spectral contrast in Figure 21(a) – notice how (as with diffuse reflection spectra recorded from some neat powders) the intensity of the weaker bands is apparently comparatively enhanced). The effects may become very pronounced for some bands in similar preparation spectra recorded from inorganic oxyanions, because of their very high absorptivities (see, for example, Figure 22). Notice, however, that in these particular spectra the asymmetry in band profile is reversed.

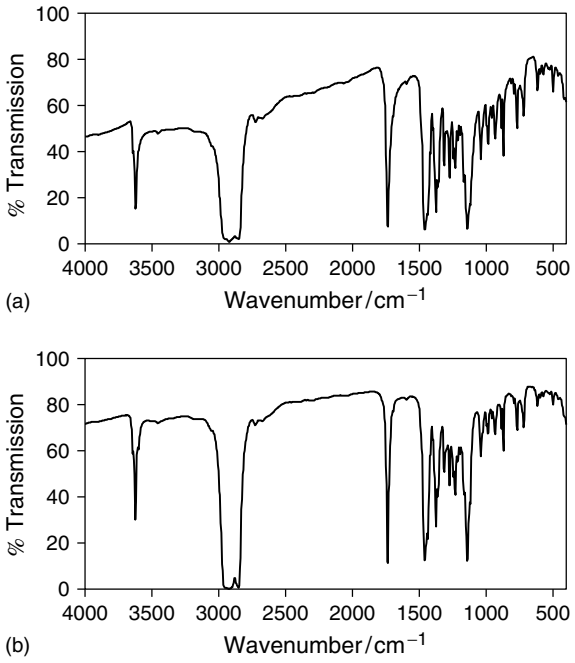

Figure 20. IR transmission spectra from an Irganox® 1010, a phenolic antioxidant, sample prepared as dispersions in liquid paraffin (Nujol®). The analyte powder sample, Irganox® 1010, was poorly ground in the mull from which the spectrum in (a) was recorded, but finely ground in the sample used to record the spectrum in (b).

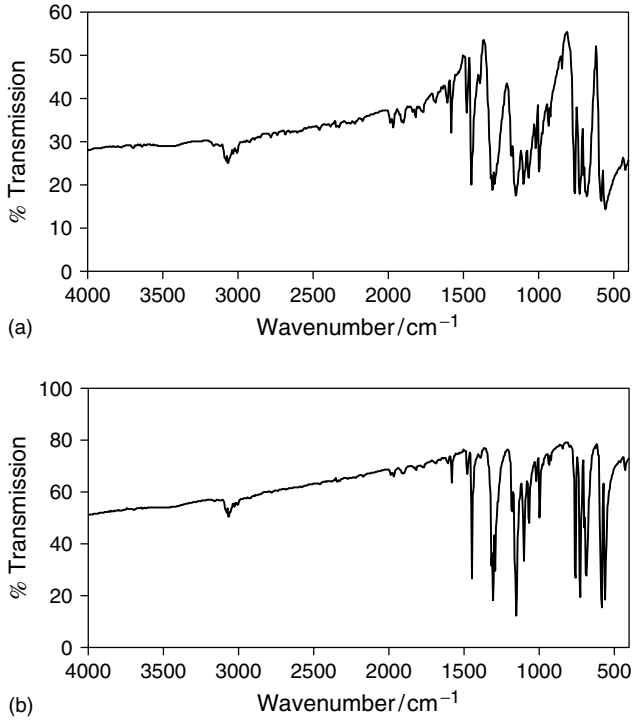

Figure 21. IR transmission spectra from a diphenyl sulfone (DPS) sample prepared as dispersions in a KBr disk. The DPS was poorly ground and not well dispersed in the disk preparation from which spectrum (a) was recorded, but was finely ground and well dispersed in the disk used to record spectrum (b).

The spectra plotted on an absorbance scale shown as Figure 23 are included as an illustration of extreme cases. They were recorded as transmission spectra from 1% w/w concentration of essentially monodisperse silica spheres prepared as KBr disks.[2] There is much similarity between these spectra and those of Figure 24, which were recorded as diffuse reflection spectra from 5% w/w dilutions of the silica spheres in ball-milled KBr.[2] In these two figures, the progression is self-evident from domination of the spectrum

Handbook of Vibrational Spectroscopy, Online © 2006 John Wiley & Sons, Ltd.

This article was published in the *Handbook of Vibrational Spectroscopy* in 2006 by John Wiley & Sons, Ltd.
DOI: 10.1002/9780470027325.s3101

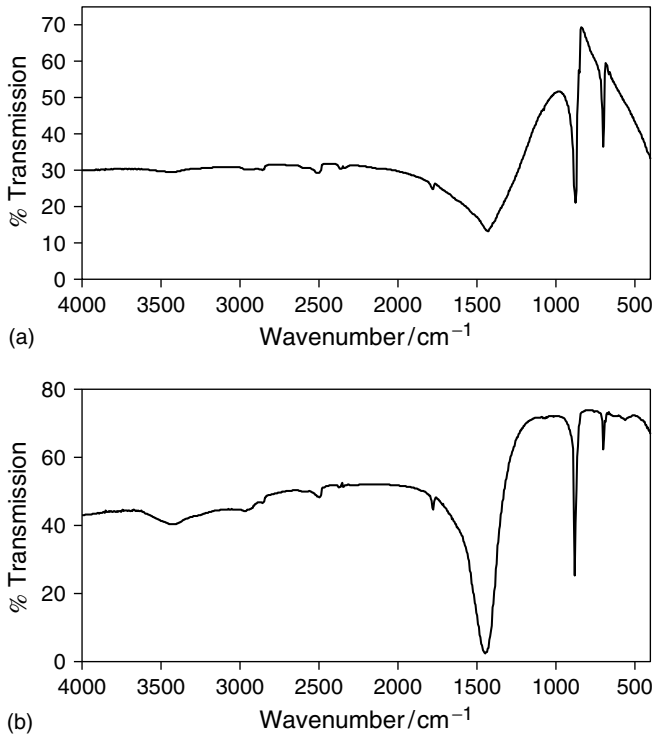

Figure 22. IR transmission spectra recorded from sodium carbonate powder prepared as dispersions in a KBr disk. The Na_2CO_3 was not ground in the disk preparation from which spectrum (a) was recorded, but was finely ground in the KBr disk used to record spectrum (b).

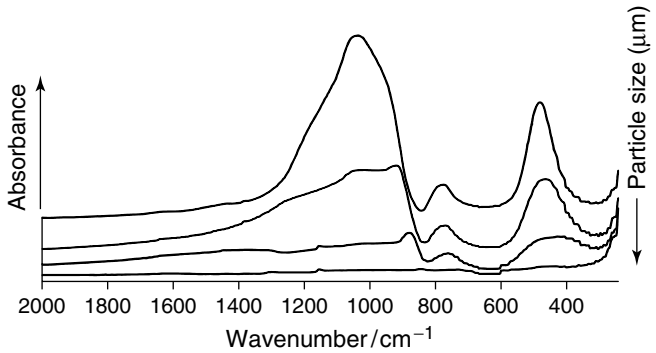

Figure 23. A series of IR absorbance spectra recorded from 1% w/w concentrations of monodisperse silica spheres prepared as KBr disks. The particle sizes of the silica spheres were 2, 8, 15 and 32 μm. [Reproduced from Ibbett (1988)[2] by kind permission of the author.]

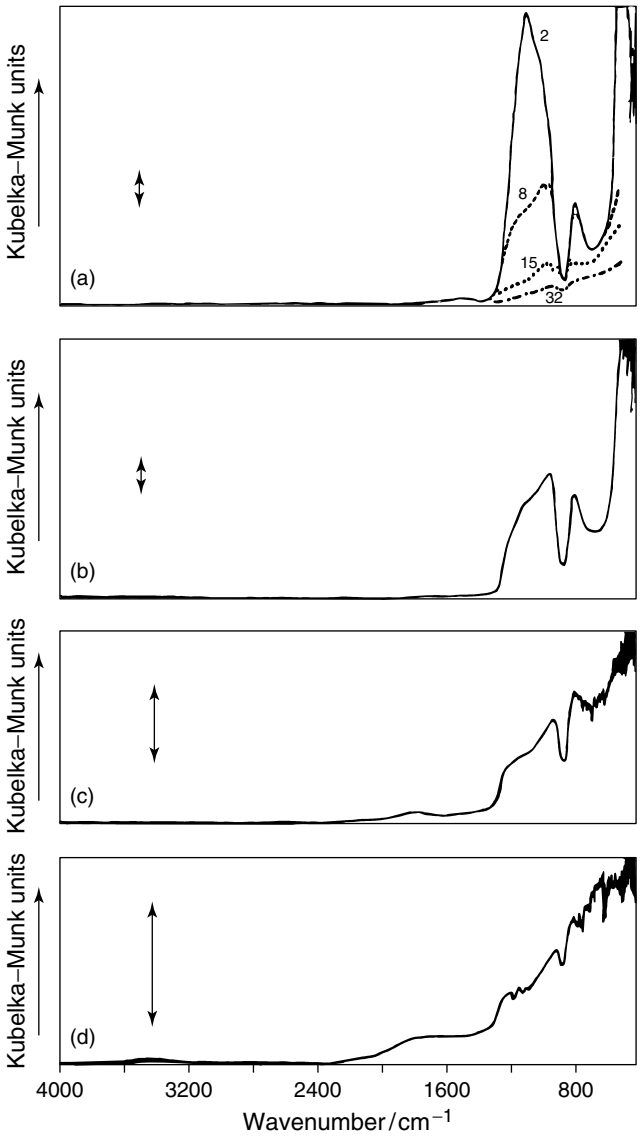

Figure 24. A series of IR diffuse reflection spectra recorded from 5% w/w concentrations of monodisperse silica spheres dispersed in ball-milled KBr powder. The particle sizes of the silica spheres were (a) 2, (b) 8, (c) 15 and (d) 32 μm. The double-headed vertical arrows indicate 2 Kubelka–Munk units. The dashed plots on (a) are for the other particle sizes plotted on the same ordinate scale. [Reproduced from Ibbett (1988)[2] by kind permission of the author.]

by absorption characteristics of the analyte at low particle size, through external reflection processes, to, at the highest particle size, radiation mostly bypassing the analyte.

Figure 25 shows as a more realistic comparison of the potential effects of particle size on diffuse reflection spectra of a neat organic material. The loss of spectral contrast and increasing interference from specular components with increasing mean particle size is clear. An even more practical comparison is given in Figure 26. This compares the spectra of DPS, as: (a) an absorbance plot from a transmission spectrum recorded from a 1% w/w KBr disk preparation; (b) a Kubelka–Munk plot from a diffuse reflection spectrum of pure ball-milled DPS; and (c) a Kubelka–Munk plot from a diffuse reflection spectrum from a 1% w/w well-dispersed mixture of ball-milled DPS diluted into ball-milled KBr. The influence of Fresnel reflection components on the most intense bands is clearly evident in Figure 26(b).

Handbook of Vibrational Spectroscopy, Online © 2006 John Wiley & Sons, Ltd.

This article was published in the *Handbook of Vibrational Spectroscopy* in 2006 by John Wiley & Sons, Ltd.
DOI: 10.1002/9780470027325.s3101

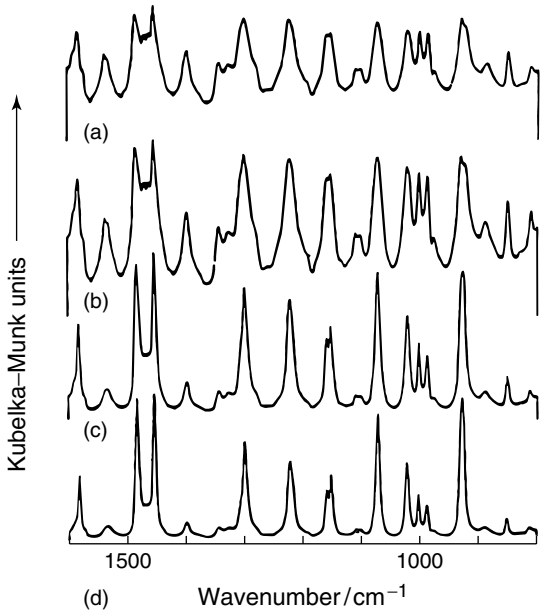

Figure 25. A series of diffuse reflection spectra recorded from neat azobenzene versus a KCl powder reference. Mean diameter, d, of the particles: (a) $d > 90\,\mu m$; (b) $75\,\mu m < d < 90\,\mu m$; (c) $10\,\mu m < d < 75\,\mu m$; (d) $d < 10\,\mu m$. [Reproduced from 'Diffuse Reflectance Measurements by Infrared Fourier Transform Spectrometry', Fuller M.P. and Griffiths P.R., *Anal. Chem.*, 1978, **50**, 13, 1906, by kind permission of the American Chemical Society, © 1978.]

In addition to particle size, packing density and compaction pressure are two more important factors that can have significant effects on diffuse reflection spectra. Figure 27 compares two diffuse reflection spectra recorded from a powder sample of 1% w/w ball-milled KNO_3 mixed with ball-milled KBr at two compaction pressures.[2] Also shown is a diffuse reflection spectrum recorded from a neat sample of the ball-milled KNO_3 at one of the compaction pressures; note the "missing" band of KNO_3 at ca. 1380 cm^{-1}in this spectrum due to the influence of front surface reflection.

8 SATURATION IN PHOTOACOUSTIC MEASUREMENTS

The prime first-order relationship that defines the relative intensities of bands within a magnitude photoacoustic Fourier transform infrared (PA/FT-IR) measurement is the ratio of the optical decay length (optical absorption depth) to the thermal wave decay length (or thermal diffusion depth). The optical absorption depth is the reciprocal of the linear absorption coefficient of a band, while the thermal diffusion depth is proportional to the thermal diffusivity. The relative magnitude of these two parameters governs the observed relative band intensities within a

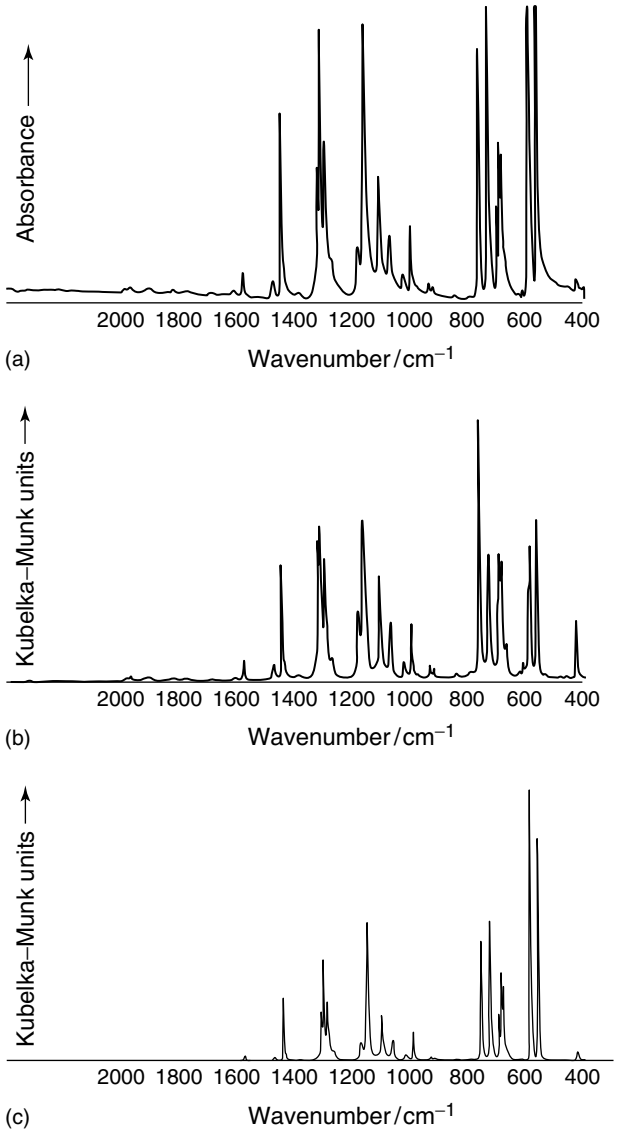

Figure 26. IR spectra of DPS. (a) Absorbance spectrum from a transmission measurement on a 1% w/w KBr disk preparation; (b) a Kubelka–Munk plot from a diffuse reflection spectrum of pure ball-milled DPS; (c) a Kubelka–Munk plot from a diffuse reflection spectrum from a 1% w/w well-dispersed mixture of ball-milled DPS diluted into ball-milled KBr. [Reproduced from Ibbett (1988)[2] by kind permission of the author.]

PA/FT-IR spectrum. For optically opaque samples, there is increasing potential for photoacoustic saturation with increasing absorptivity. This manifests itself initially as a deviation from linearity with either concentration or absorptivity until at high absorptivities (or with increasing sample thickness) full saturation occurs, such that no further increase in signal is observed with increasing concentration or absorptivity. For an optically thick homogeneous sample, the effects of saturation become lessened with increasing modulation frequency, since the effective sample thickness investigated becomes thinner. The theory and consequences

Handbook of Vibrational Spectroscopy, Online © 2006 John Wiley & Sons, Ltd.

This article was published in the *Handbook of Vibrational Spectroscopy* in 2006 by John Wiley & Sons, Ltd.
DOI: 10.1002/9780470027325.s3101

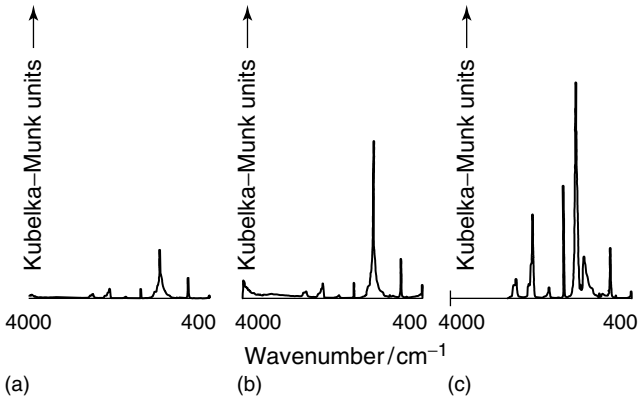

Figure 27. Diffuse reflection spectra of ball-milled KNO_3. (a) and (b) 1% w/w ball-milled KNO_3 dispersed in ball-milled KBr at compaction pressures of ~17.5 kPa and ~520 kPa, respectively; (c) neat ball-milled KNO_3 at compaction pressure of ~520 kPa. (a) and (b) are on the same ordinate scale; the ordinate scale expansion of (c) is 1/25 that of the scale for (a) and (b). [(a, b) Reproduced from Ibbett (1988)[2] by kind permission of the author. (c) was also reproduced by kind permission of Roger Ibbett.]

of these effects and others are discussed fully elsewhere in this handbook (see **Photoacoustic Spectroscopy**).

9 DIFFRACTION IN FT-IR MICROSCOPY MEASUREMENTS

The last decade of the twentieth century saw FT-IR microscopy become a technique of widespread usage and maturity. Instrumentation is now a common feature in many industrial, biomedical and forensic analytical laboratories, covering diverse application areas, many of which are featured within the pages of this handbook. The technique is also an important tool for many academic research studies. Over this decade there has, however, been considerable discussion and debate about the ultimate in lateral spatial resolution that may be achieved in an FT-IR microscopy transmission measurement. To a first approximation, the spatial resolution of a FT-IR microscope is approximately equal to the wavelength of the radiation. As a result, the one-dimensional values commonly quoted for the lateral spatial resolution of an FT-IR microscope have varied from about 5 μm through to 10 μm or even 15 μm. It will depend on the wavelengths being examined; the spatial resolution will be better at shorter wavelengths.

In the mid-infrared, using a narrow band cooled mercury cadmium telluride (MCT) detector, the spectral range scanned is normally about 4000–650 cm^{-1}. This represents a wavelength range of about 2.5–15.5 μm. In a conventional FT-IR microscopy system using an incandescent source, such as a Globar® or similar, then the lower values commonly pronounced for spatial resolution purport to the fact that it is possible to record an IR spectrum through an aperture of such a dimension. The higher values represent situations where a mid-infrared spectrum essentially free of diffraction-induced artifacts may surely be recorded. (For a low-divergence, high-brightness IR source, such as that emanating from a synchrotron, the lateral spatial resolution is often perceived as better, since most of the radiation may be focused to a spot of diameter about 10 μm. Synchrotron-sourced IR FT-IR microscopy spectra have been reported recorded through a 3 μm × 3 μm square aperture.) The key for the spectrum interrogator is how pure is the recorded spectrum, is it really only from material within the sample area defined by the delimiting aperture, or is there any intrusion of spectral features from surrounding areas? Radiation will certainly pass through an aperture significantly narrower than its wavelength, but it will suffer considerable diffraction. (Diffraction theory, diffraction patterns and the diffraction limit, particularly for point sources, are covered extensively in many physics textbooks, and the situation with respect to optimizing IR microscope design and practice has been addressed by Messerschmidt,[3] and by Sommer in **Mid-infrared Transmission Microspectroscopy** in this handbook.) The source and focusing optics provide a range of incidence angles, and the sample and its support, if there is one, will likely induce significant refraction, maybe some diffuse transmission. In truth, there is probably no absolute answer to the question of what is the ultimate spatial resolution in practice. It will be, at least, both sample and wavelength dependent. It is the opinion of this author that for a conventional FT-IR microscopy set-up, it will likely be realized practically as being in the region of 8–10 μm.

As a practical illustration, Figure 28 represents an example of a well-publicized industrial application of FT-IR microscopy, namely that of characterizing the layers in a polymer laminate, by examining in transmission sequential layers of a cross-section microtomed from the sample. The spectra recorded from both the 50 μm wide polypropylene and 10 μm wide polyester (PET) layers are good matches against appropriate standard reference spectra of the two materials. However, the spectrum recorded from the approximately 8 μm wide polyurethane (adhesive) layer shows absorption features associated with both the surrounding layers, which intrude more with increasing wavelength (decreasing wavenumber). A similar examination is shown in Figure 29(a), this time from a polyurethane adhesive layer between two PET films. The spectrum recorded of the adhesive layer from a free-standing cross-section clearly shows many absorption features associated with PET. For comparison, an FT-IR microscopy spectrum recorded from the adhesive layer of the cross-section after it had been squashed in a diamond window compression cell is shown also in Figure 29(b). The compression increased

Handbook of Vibrational Spectroscopy, Online © 2006 John Wiley & Sons, Ltd.

This article was published in the *Handbook of Vibrational Spectroscopy* in 2006 by John Wiley & Sons, Ltd.
DOI: 10.1002/9780470027325.s3101

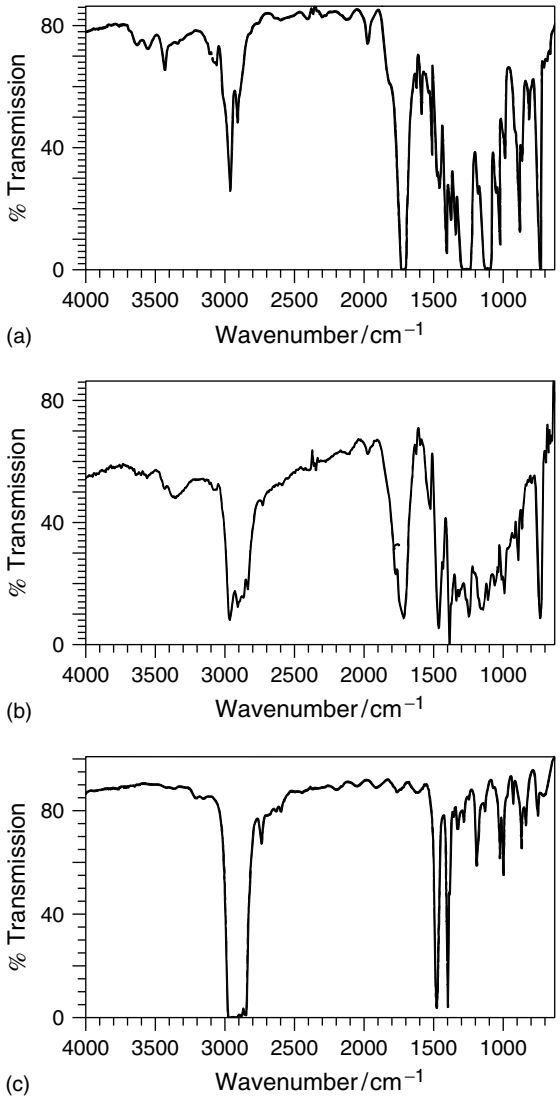

Figure 28. FT-IR microscopy transmission spectra of three consecutive layers of a thin transverse section cut (microtomed) from a multilayer polymer laminate: (a) 50 µm wide polypropylene layer; (b) ~8 µm wide layer showing the likely presence of a polyurethane (adhesive) layer plus intrusion of spectral features from the surrounding layers; (c) 10 µm wide polyester layer. [Reproduced from Chalmers J.M., Croot L., Eaves J.G., Everall N., Gaskin W.F., Lumsdon J., Moore N., *Spectrosc. Int. J.*, **8**, 13 (1990) by kind permission of IOS Press, Amsterdam.]

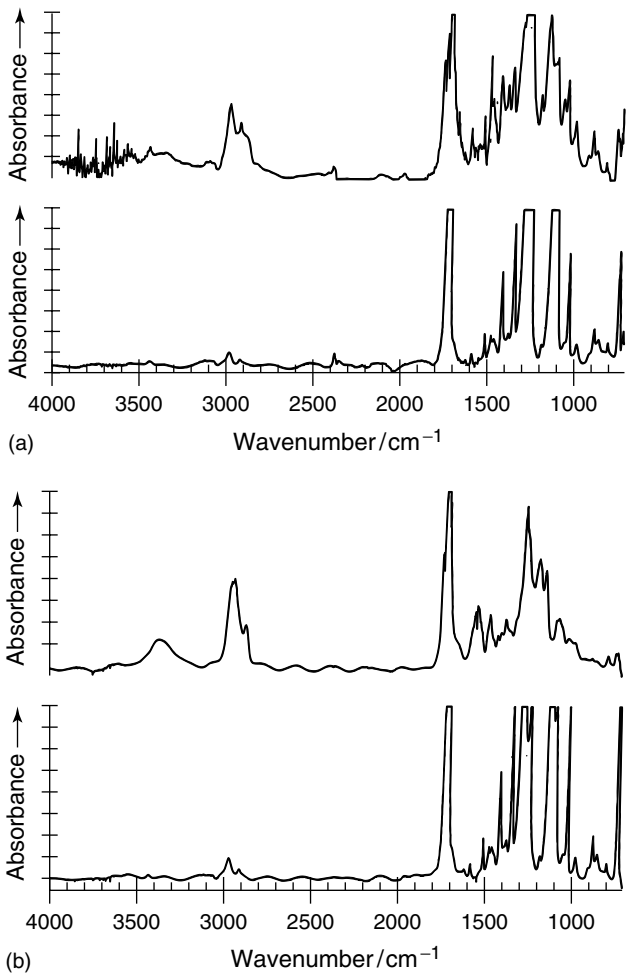

Figure 29. (a) FT-IR microscopy absorbance spectra from transmission measurements of adjacent layers in a thin cross-section (microtomed) from a multilayer film, the composition of which was PET/adhesive/PET. (b) FT-IR microscopy absorbance spectra from transmission measurements of adjacent layers in the thin cross-section (microtomed) from a multilayer film used in (a) after it had been squashed in a diamond window compression cell.

the width of the softer polyurethane layer to an extent that a "pure" spectrum could be recorded that was characteristic of the adhesive.

10 DETECTOR NON-LINEARITY – BEER'S LAW

It is generally accepted that in the mid-infrared region room temperature detectors, such as the DTGS (deuterated triglycine sulfate), are presently more linear than the more sensitive cooled detectors, such as MCT. Also, to obtain the best linearity, it is not advisable in quantitative analysis to perform measurements on bands of absorbance greater than 0.7 (equivalent to a peak maximum of about 20% transmission), and certainly not greater than 1.0. This rule of thumb is particularly important if triangular apodization is being applied. Non-linearity (non-photometric accuracy) in detector response manifests itself as a curved calibration graph (deviation from a Beer's law plot). The problem becomes more acute as the band being measured becomes narrower. Software of many FT-IR spectrometer systems will display and plot absorbance scales to values of 4 or 8, and sometimes even higher; thus, it is worth recalling that absorbance values of 3 and 4 correspond to only 0.1% and 0.01% transmission, respectively. Thus the signal-to-noise

Handbook of Vibrational Spectroscopy, Online © 2006 John Wiley & Sons, Ltd.

This article was published in the *Handbook of Vibrational Spectroscopy* in 2006 by John Wiley & Sons, Ltd.
DOI: 10.1002/9780470027325.s3101

ratio may be very low near the center of strong absorption bands and the photometric accuracy of many contemporary FT-IR spectrometers is only ±0.1% T. More detailed discussion on the effects of photometric accuracy on Beer's law plots can be found in **Beer's Law** by Griffiths in this handbook.

For very weak bands, the quantitative accuracy is given by a number of parameters, including the noise level on the spectral baseline, the baseline flatness, the level of impurities in the sample, and how well atmospheric H_2O and CO_2 have been compensated.

11 POLYMORPHIC AND MORPHOLOGICAL CHANGES, METASTABLE AND ENVIRONMENT/TIME DEPENDENT STATES

Many solid materials exhibit polymorphism, and some form changes are accompanied by very significant differences between their associated vibrational spectra. Some states may also be metastable, reverting in time to a more stable form, again leading to changes in the IR spectrum of the material. Other equilibrium states may be altered by the method of sample presentation, containment or preparation. Clearly, many such changes may be invoked deliberately or anticipated through variations in experimental parameters, such as temperature or pressure, but the few examples mentioned in this section all occurred at room temperature using conventional methods of sample analysis. It is hoped that they serve to illustrate some, perhaps unanticipated, consequences of analysing a sample by IR spectroscopy. In all cases the IR spectrum changed with time.

Polymorphism and its effects on vibrational spectra, particularly compounds of interest to the pharmaceutical industry, are discussed in detail in **Polymorphs, Solvates and Hydrates** in Volume 5 of this handbook. Also, examples of spectral changes resulting from different crystal forms of organic polymers may be found in the Volume 3 article **Spectra–Structure Correlations: Polymer Spectra**. Two examples relevant to this part of our discussion may be found in **Spectra–Structure Correlations: Polymer Spectra** as Figures 12 and 18 and their associated texts. The first concerns desorption of water from a polymer film while it is mounted in the IR beam in the sample compartment of an IR spectrometer (see Figure 12 of **Spectra–Structure Correlations: Polymer Spectra**). The peculiarity here is that the water that was in equilibrium with the polymer film gave rise to νOH stretching bands at 3650 cm^{-1} and 3550 cm^{-1}. The presence of the band at higher wavenumber implied entrapment of isolated (non-hydrogen-bonded) water molecules within the polymer matrix.

The second example from **Spectra–Structure Correlations: Polymer Spectra** covers changes between the common polymorphic forms of polybutene. A polybutene film prepared from the melt will likely exist in the type II crystalline modification, but with time it reverts to the higher-density type I form. This change, which may take place over a several days, is accompanied by steady but significant changes in the absorption pattern in the fingerprint region of the spectrum (see Figure 30) (also, see Figure 18 of **Spectra–Structure Correlations: Polymer Spectra**).

The third example selected shows how different thermal histories may affect the state of a dispersed material. Figure 31 shows IR spectra over the range 1700–1400 cm^{-1} recorded from calcium stearate (CaSt) in three different sampling presentations.[4] The absorbance spectra generated from a transmission measurement of CaSt as a dispersion in a KCl disk and the Kubleka–Munk plot of powdered

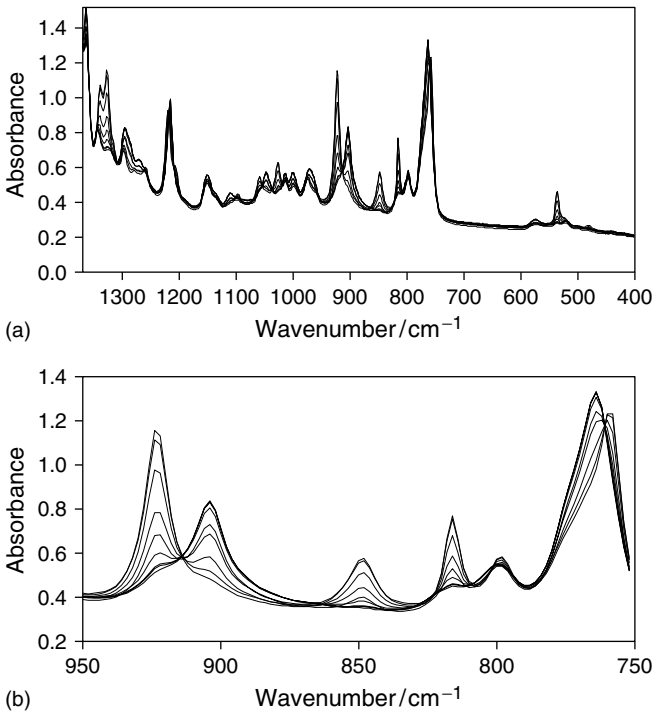

Figure 30. (a) Nine overlaid IR, 4 cm^{-1} resolution, spectra recorded from a polybutene film over a period of about 3 days, during which time it reverted from a type II to a type I crystalline form. (b) Scale-expanded plot over the range 950–750 cm^{-1} of the plots shown in (a), showing the increase with time of absorptions at 923 cm^{-1}, 848 cm^{-1} and 816 cm^{-1}, an absorption decrease with time at 903 cm^{-1}, and an apparent shift in band maximum with time from 763 cm^{-1} to 758 cm^{-1}. The time intervals between when a spectrum was recorded after the initial spectrum was taken were 11, 20, 62, 135, 345, 512, 2660 and 4196 min.

Handbook of Vibrational Spectroscopy, Online © 2006 John Wiley & Sons, Ltd.

This article was published in the *Handbook of Vibrational Spectroscopy* in 2006 by John Wiley & Sons, Ltd.
DOI: 10.1002/9780470027325.s3101

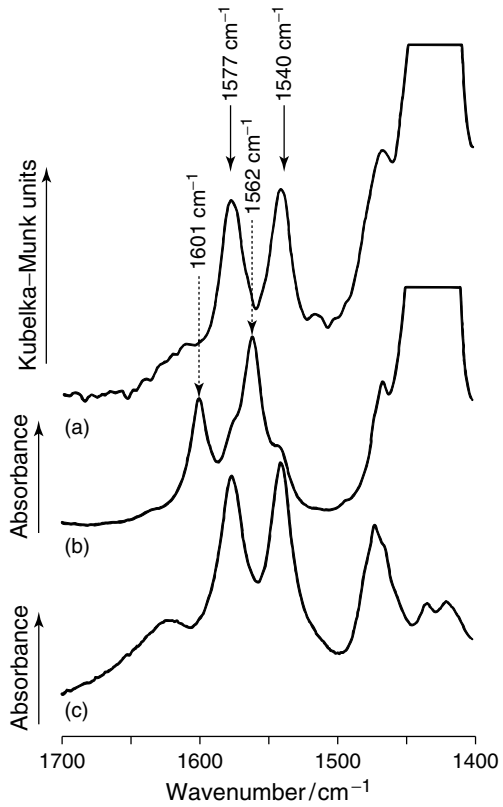

Figure 31. (a) Diffuse reflection spectrum of CaSt dispersed in powdered KCl; (b) absorbance spectrum of CaSt stabilized PVC film; (c) absorbance spectrum of CaSt in a KCl disk preparation. [Reproduced by permission from J.M. Chalmers, M.W. Mackenzie and H.A. Willis, *Appl. Spectrosc.*, **38**, 763 (1984).]

PVC containing CaSt, as a stabilizer, dispersed in powdered KCl generated from a diffuse reflection measurement, both exhibit CaSt bands with maxima at 1577 cm^{-1} and 1540 cm^{-1}. However, these bands appear at 1601 cm^{-1} and 1562 cm^{-1} in a transmission measurement recorded from a sample of the stabilized PVC powder prepared as compression molded (hot pressed) film from the melt. The bands at 1601 cm^{-1} and 1562 cm^{-1} are attributed to a metastable form of CaSt, since in time the CaSt reverted slowly to the more stable crystalline form, with a consequent shift of the bands to 1577 cm^{-1} and 1540 cm^{-1}.

The final example in this section shows morphological changes induced into a sample of PEEK while contained under pressure in a diamond window compression cell. The analysis concerned examining by FT-IR microscopy a visible small defect area in a PEEK molding. The defect was isolated from the molding and compressed between the windows of a diamond compression cell to facilitate analysis by FT-IR microscopy. The resultant spectrum showed readily that the defect area had a different morphology to the bulk material of the molding, in that it was amorphous. However, over about 2 days the contained sample underwent pressure-induced crystallization, as evidenced by changes in its spectrum (Figure 32). Its spectrum then looked very similar to that recorded from the crystalline bulk material, such that the spectrally observed physical difference information between the defect and the bulk material was lost!

Many materials may undergo morphological or state changes, such as pressure-, temperature- or solvent-induced crystallization, with time or as a consequence of differing histories or containment environments. Most of these physical changes will be reflected by changes in the materials' IR spectrum that may be considerable. The few examples here emphasize the fact that an IR spectrum of a sample represents the fingerprint of that sample in its physical state and environment the time the spectrum was recorded, and not just its perceived chemical structure.

12 INVERTED BANDS IN EMISSION SPECTRA

Mid-infrared emission studies are mostly limited to examining thin specimens or a thin layer/film on a weakly absorbing substrate. Typical of these might be an adsorbed species on a catalyst surface or a coating on a beverage

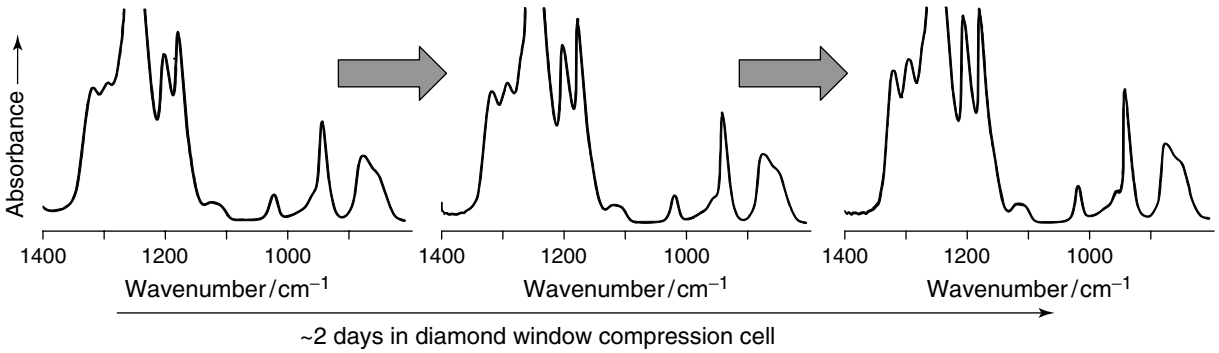

Figure 32. IR absorbance spectra recorded from an FT-IR microscopy transmission measurement of a defect isolated from a PEEK molding. The defect was flattened and contained under pressure in a diamond window compression cell.

Handbook of Vibrational Spectroscopy, Online © 2006 John Wiley & Sons, Ltd.

This article was published in the *Handbook of Vibrational Spectroscopy* in 2006 by John Wiley & Sons, Ltd.
DOI: 10.1002/9780470027325.s3101

can, that is regimes where it is possible to generate a spectrum that is characteristic of the fingerprint pattern associated with the analyte. Although the use of IR emission spectroscopy as an analytical tool has become sparser with the arrival of FT-IR sampling techniques such as PA and diffuse reflection, in an article such as this, it is worth noting a few oddities. The theory, sample handling and applications of IR emission spectroscopy together including some discussion of spectral distortions may be found in **Infrared Emission Spectroscopy** by Mink in this handbook.

In optically opaque samples it is possible to observe apparently inverted bands in their emission spectra. These distortions arise from re-absorption by a colder surface layer of radiation originating from within the bulk of a sample. Mink (see **Infrared Emission Spectroscopy**) has discussed and illustrated (see Figures 7 and 8 in **Infrared Emission Spectroscopy**) some characteristics of self-absorption. Also discussed for organic materials were the so-called "reduced emission" phenomena (see, for example, Sheppard[5]), at wavenumbers where significant front surface reflection occurs.

The wavenumber dependent absorptance (α) of a sample is given as:

$$\alpha = 1 - (t + r) \tag{1}$$

where t and r represent the transmittance and reflectance of the sample, respectively.

The equivalent expression for emission spectrometry, through Kirchhoff's law, in terms of a sample's emissivity (ε) is:

$$\varepsilon = 1 - (t + r) \tag{2}$$

Remembering that there is dispersion in the refractive index as one traverses an absorption band (see preceding section), then there is therefore an equivalence in the case of emittance. Figure 33 shows an example of "reduced emission" observed in the emission spectra of a series of PET films of differing thickness.[5] Band splitting is clearly observed on the νC=O band at ca. 1725 cm^{-1} in Figure 33(a). Loss of spectral contrast is clearly seen in the emission spectrum of Figure 33(b), as the more intense bands approach saturation (see **Infrared Emission Spectroscopy**). The minima observed at 1725 cm^{-1} and 1265 cm^{-1}in Figure 33(c), may be explained by the effect of "reduced emission", while the minima in the vicinity of 1900 cm^{-1} and 600 cm^{-1} are genuine regions of low emissivity.[6]

In the case of organic polymers, optical opacity may be the consequence of a high level of a filler material, such as carbon black, rather than as a result of absorption because of an excessive sample thickness. Spectra recorded from such samples may also show inverted spectra, but in this instance not as a consequence of selective reflection. In these cases, filler material may act as a relatively efficient blackbody emitter, that is, as a conventional source for the surrounding polymer matrix, which being cooler absorbs at its characteristic frequencies. Examples of such an effect may be seen in the spectra of Figure 34. The features within the emission spectrum recorded will depend not only on the sample temperature, but also on the filler level and its dispersion, the film thickness, the thermal balance between the filler and the polymer, and the wavelength dependence of the Planck function. (More detailed discussion of this and further examples may be found in Chalmers and Mackenzie.[6])

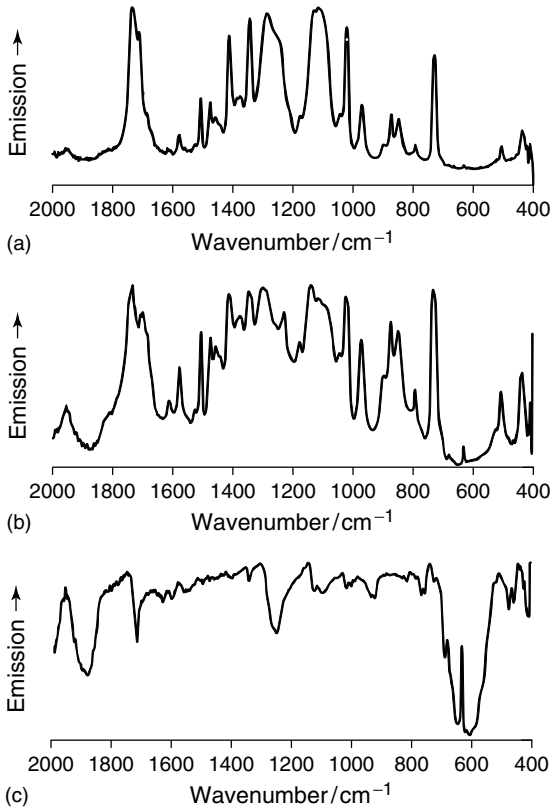

Figure 33. IR, 4 cm^{-1} resolution, emission spectra recorded at 348 K from a series of PET films: (a) 2.5 µm thick; (b) 9 µm thick; (c) 100 µm thick. [Reproduced from J.M. Chalmers and M.W. Mackenzie, 'Solid Sampling Techniques', in M.W. Mackenzie (ed.), "Advances in Applied Fourier Transform Infrared Spectroscopy", J. Wiley & Sons, Chichester, 105–188 (1988). Copyright 1988. ©John Wiley & Sons Limited. Reproduced with permission.]

13 EXTERNAL REFLECTION – MIXED-MODE SPECTRA

In recent years, increased analytical use has been made of external reflection as a convenient sampling technique,

Handbook of Vibrational Spectroscopy, Online © 2006 John Wiley & Sons, Ltd.

This article was published in the *Handbook of Vibrational Spectroscopy* in 2006 by John Wiley & Sons, Ltd.
DOI: 10.1002/9780470027325.s3101

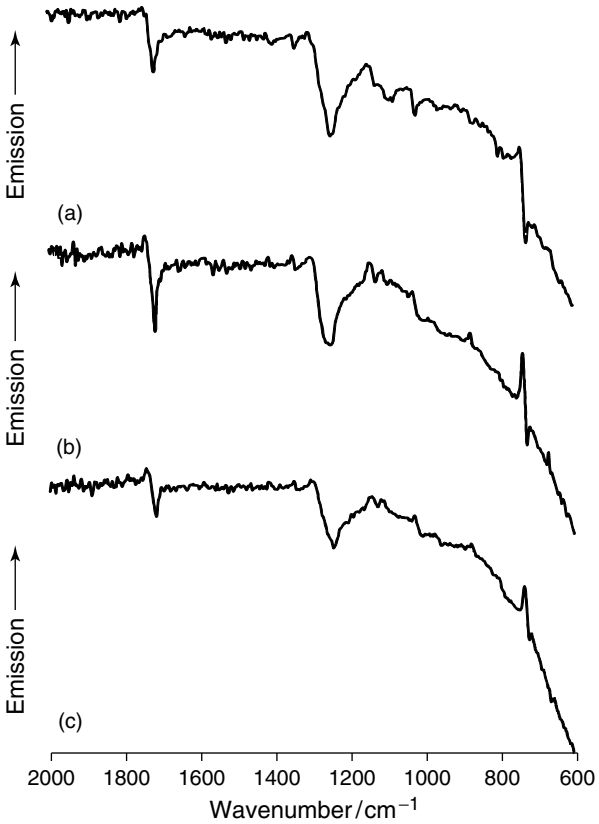

Figure 34. IR, 4 cm^{-1} resolution, emission spectra recorded at 348 K from a series of 20% carbon-black-filled PET films: (a) 150 μm thick; (b) 10 μm thick; (c) 5 μm thick. Spectra have been offset for clarity. [Reproduced from J.M. Chalmers and M.W. Mackenzie, 'Solid Sampling Techniques', in M.W. Mackenzie (ed.), "Advances in Applied Fourier Transform Infrared Spectroscopy", J. Wiley & Sons, Chichester, 105–188 (1988). Copyright 1988. ©John Wiley & Sons Limited. Reproduced with permission.]

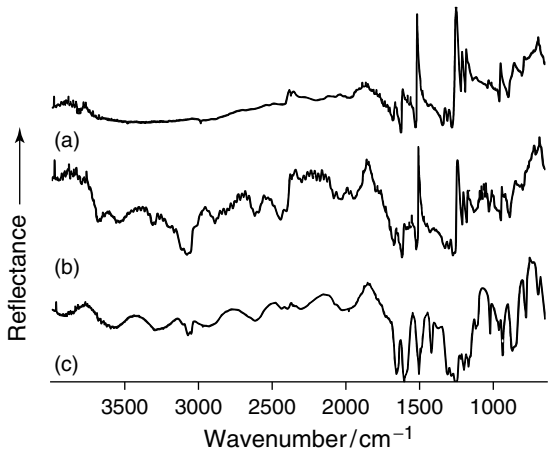

Figure 35. FT-IR microscopy, external reflection spectra recorded from a series of PEEK samples: (a) 3 mm thick; (b) 125 μm thick; (c) 10 μm thick.

particularly in combination with FT-IR microscopy measurements. The benefit has been derived from the ready application of the K–K transformation of Fresnel reflection spectra to the optical constants of the sample, and thereby extracting the analytically useful absorption index spectrum. Successful application of this approach depends on the purity of the front-surface reflection spectrum. The sample must be optically flat, homogeneous, and optically thick. If the sample form does not meet these requirements, then a "mixed-mode" spectrum may be recorded that is useless for such a treatment. As an example, Figure 35 shows IR spectra recorded from three samples of the same polymer, each of a different thickness, from a front-surface reflection experimental arrangement. Neglecting the features due to atmospheric water vapor and CO_2, the spectrum from the thickest sample (3 mm thickness) is what is expected from a front-surface reflection measurement and appropriate for K–K treatment. The spectrum recorded from the thinnest sample (a 10 μm thick film) is dominated by absorption features and resembles that recorded from a transflection measurement, but on which is superimposed an interference fringe pattern. This is because the dominant features arise from radiation that has been transmitted through the sample and then been reflected back from the films' lower surface, but attenuated by the characteristic absorption bands of the sample. At high wavenumber (short wavelength), the middle spectrum, from a film of 125 μm thickness, has similar character to the spectrum recorded from the thinnest film, but with a different fringe frequency. However, at low wavenumber the spectrum more resembles a true, front-surface reflection spectrum, particularly in the vicinity of bands with high absorptivities. Clearly, neither of the spectra recorded from the two thinner samples is in a form appropriate to a K–K transform approach.

14 SCALE EXPANSION: DIGITIZATION STEPS AND PLOT SOFTWARE CHARACTERISTICS

The number of data points in a mid-infrared recorded interferogram relates to the resolution at which the desired spectrum is to be analyzed. The point density in the transformed spectrum may possibly be increased by an integer multiplication of the number of recorded data points, depending on the level of zero-filling chosen. When the spectrum is plotted with high abscissa expansion, the spectrum may appear disjointed, being composed as a series of points connected by straight lines. Some plot software algorithms further increase the point density (not the spectral resolution though) through interpolation, by, for example, fitting polynomials through successive blocks of data points. Like zero-filling, spline interpolation serves

Handbook of Vibrational Spectroscopy, Online © 2006 John Wiley & Sons, Ltd.

This article was published in the *Handbook of Vibrational Spectroscopy* in 2006 by John Wiley & Sons, Ltd.
DOI: 10.1002/9780470027325.s3101

primarily as an aesthetic function implemented to improve band contour; the spectral resolution is implicit and defined by the non-zero-filled interferogram.

15 SINGLE-BEAM BACKGROUND CHOICE

The choice of single-beam background for measuring a sample's FT-IR spectrum should be that which most closely represents the conditions under which the sample's single-beam spectrum is recorded. For example, if an accessory such as an internal reflection unit is used, then the background spectrum should be taken through the same unit in the same alignment in the sample compartment fitted with the internal reflection element to be used, but without the sample. This consideration, of matching as closely as possible the throughput and light paths under which the two single-beam spectra are recorded, will minimize artifacts and distortions in the sample's spectrum.

As a trivial example of minimizing such distortions, the spectra of Figure 36 may be compared. The pair of spectra were recorded from a polysulfone film of about 10 μm thickness. The film was mounted in a 25 mm × 11 mm aperture card sample mount. In Figure 36(a), the single-beam background used was that of the open beam. The mismatch in beam dimensions between the two ratioed single-beam spectra, produced the sloping background and overall reduced transmission scale for the sample spectrum. To compensate for the vignetting caused by the sample card mount, the single-beam background spectrum for Figure 36(b) was recorded through an empty aperture sample mount located as near as possible in the same position, in the sample compartment at the beam focus, as for that used to record the sample single-beam spectrum. The improvement in spectral integrity is self-evident.

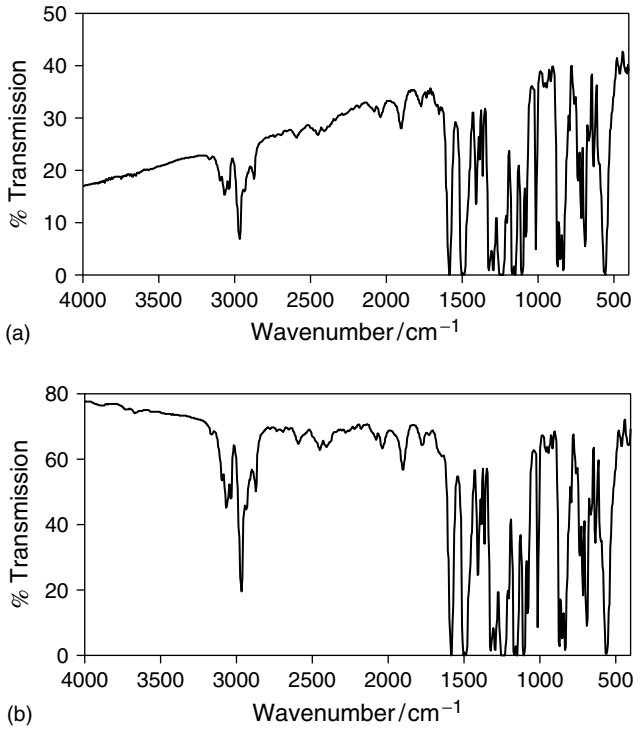

Figure 36. IR, 4 cm^{-1} resolution, transmission spectra recorded from a polysulfone film. The film was mounted in the 25 mm × 11 mm aperture of a sample card mount. The single-beam background spectrum used for (a) was the unrestricted spectrometer open beam, while that for (b) was an open beam but with an empty card mount sited in the sampling position.

16 DATA MANIPULATION AND TREATMENT

Many artifacts or distortions may be introduced into spectra as a consequence of data treatment or manipulation by software algorithms. Some, such as phase correction considerations in high-resolution spectra, are beyond the scope of this article. Others, such as decreasing signal-to-noise ratio with increasing levels of deivatization, loss of spectral contrast and detail with smoothing, or introduction of side lobes in Fourier self-deconvolution, have been discussed in the appropriate articles within this handbook.

Spectral subtraction (difference spectroscopy) is a manipulation that is both extremely valuable and seriously open to abuse in the interpretation of its results. It should always be undertaken between two absorbance or two absorbance-equivalent spectra, e.g. Kubelka–Munk, absorption index or photoacoustic intensity plots. It is not uncommon to observe within an appropriately factored difference spectrum features that may indicate a band shift, a band narrowing, a band increase or an increase or decrease in band intensity. At high ordinate scale expansions, similar effects can sometimes arise as artifacts, and not be associated with real changes. For instance, assuming there are no time-dependent changes, then such artifacts can appear in a difference spectrum generated by subtracting two absorbance spectra generated from consecutively recorded spectra from the same sample, but where the sample was merely removed from and then replaced into the sample compartment beam between the recordings.

17 INSTRUMENT

Up to this point, the discussion in this article has concentrated mostly on anomalies, artifacts and errors arising out of sample preparation and presentation and spectral display. This has been deliberate, since in mid-infrared measurements, these are the most common sources of malpractice

Handbook of Vibrational Spectroscopy, Online © 2006 John Wiley & Sons, Ltd.

This article was published in the *Handbook of Vibrational Spectroscopy* in 2006 by John Wiley & Sons, Ltd.
DOI: 10.1002/9780470027325.s3101

associated with measurements made on condensed phases at spectral resolutions of 1 cm^{-1} or lower. Instrumental artifacts, such as vignetting and aliasing, leading to wavenumber shifts and spectral folding respectively, are mentioned in another article (see **Anomalies and Artifacts in Raman Spectroscopy**) in considerations of anomalies appropriate to Fourier transform (FT)-Raman spectra. These and other performance and design criteria, such as mirror alignments, and roll, tilt, yaw and shear elimination or compensation during interferometer mirror travel, become much more pertinent to more specialized applications, such as high-resolution spectroscopy, and will not be discussed here. For most commercial FT spectrometers designed today for operating in the mid-infrared region, they are of no apparent consequence to the user, except for all but the most sensitive measurements, and of no real concern for applications by conventional sampling methods undertaken at low or moderate spectral resolutions.

A classified list of 50 categories of potential ordinate error in FT spectroscopy has been published with comments by Birch and Clarke.[7] The classifications are: non-ideal spectrophotometer properties, interaction of non-ideal instrument and sample properties, effects of non-ideal properties of the sample, and deficiencies of the measurement procedures. More recently, these authors have published a preliminary appraisal of the interreflection errors in FT spectroscopy.[8] Discussions on component specifications and design and performance requirements for FT-IR spectrometers may be found in many other publications.[9–11] Some such as the Zachor–Aaronson distortion, related to non-constant mirror scan velocity, become more needy of consideration in problematic environments, such as process installations.[12]

A detailed early look at the problems involved in quantitative FT-IR by Tomas Hirschfeld was published in 1979.[13] In mid-infrared dispersive spectrometry, the inherent polarization in gratings was an important consideration. However, the effect is significantly weaker in FT-IR spectrometers (see **Mid-infrared Spectroscopy of the Condensed Phase** and Griffiths *et al*.[11] and Hirschfeld[13]). And, while the reflectance and transmittance of beam-splitters may be quite different for the two (horizontal and vertical) polarizations, the efficiency is usually quite close to unity.

18 CLOSING REMARKS

As one progresses through composing an article like this, one tends to recall (unfortunately!) examples of many instances one has experienced or observed where nuisances and nuances have occurred that resulted in spectral distortions and artifacts in mid-infrared spectra. Those that have been shared will hopefully make newcomers to the field more aware of the potential hazards associated with poor experimental practice, short-cutting well-established methodologies or attempting to circumvent (violate!) the laws of optical physics. The emphasis in this article has been deliberately biased towards sample presentation techniques, since in general practice, this is the area most prone to misconception, misunderstanding, misuse and error. This is perhaps in contrast to the article on anomalies and artifacts in Raman spectroscopy (see **Anomalies and Artifacts in Raman Spectroscopy**), for which the tendency out of necessity is more towards the instrumentation and its parameters. However, I would recommend that anyone new to the field of vibrational spectroscopy read both these articles, and also the article covering anomalies in near-infrared spectroscopy (see **Anomalies in Near-infrared Spectroscopy**). Each contains differing insights to the problems faced in recording high-quality spectra free from artifacts and distortions, and collectively they should provide a good base for developing successful approaches to both qualitative and quantitative vibrational spectroscopy practice.

ABBREVIATIONS AND ACRONYMS

CaSt	Calcium Stearate
DPS	Diphenyl Sulfone
K–K	Kramers–Kronig
PA/FT-IR	Photoacoustic Fourier Transform Infrared
PDMS	Poly(dimethyl siloxane)
PEEK	Poly(aryl ether ether ketone)
PES	Poly(aryl ether sulfone)
PET	Poly(ethylene terephthalate)
PVC	Poly(vinyl chloride)

REFERENCES

1. B.A. Macdonald (ed.), 'Chambers Twentieth Century Dictionary', W & R Chambers Ltd., Edinburgh (1979).
2. R.N. Ibbett, PhD thesis, University of East Anglia, Norwich (1988).
3. R.G. Messerschmidt, 'Minimizing Optical Nonlinearities in Infrared Microspectroscopy', in "Practical Guide to Infrared Microspectroscopy", ed. H.J. Humecki, Marcel Dekker, Inc., New York, 3–39 (1995).
4. J.M. Chalmers, M.W. Mackenzie and H.A. Willis, *Appl. Spectrosc.*, **38**(6), 763 (1984).
5. N. Sheppard, 'The Use of Fourier Transform Methods for the Measurement of Infrared Emission Spectra', in "Analytical Applications of FTIR to Molecular and Biological Systems", ed. J.R. Durig, D. Reidel, Dordrecht, 125–140 (1980).
6. J.M. Chalmers and M.W. Mackenzie, 'Solid Sampling Techniques', in "Advances in Applied Fourier Transform Infrared

Handbook of Vibrational Spectroscopy, Online © 2006 John Wiley & Sons, Ltd.

This article was published in the *Handbook of Vibrational Spectroscopy* in 2006 by John Wiley & Sons, Ltd.
DOI: 10.1002/9780470027325.s3101

Spectroscopy", ed. M.W. Mackenzie, J. Wiley & Sons, Chichester, 105–188 (1988).

7. J.R. Birch and F.J.J. Clarke, *Spectrosc. Eur.*, **7**(4), 16 (1995).
8. J.R. Birch and F.J.J. Clarke, *Anal. Chim. Acta*, **380**, 369 (1999).
9. R. Geick, *Top. Current Chem.*, **58**, 75 (1975).
10. S.F. Johnston, 'Fourier Transform Infrared Spectrometry. A Constantly Evolving Technology', Ellis Horwood, Chichester (1991).
11. P.R. Griffiths and J.A. de Haseth, 'Fourier Transform Spectrometry', J. Wiley & Sons, Inc., New York (1986).
12. D.W. Vidrine, 'Mid-infrared Spectroscopy in Chemical Process Analysis', in "Spectroscopy in Process Analysis", ed. J.M. Chalmers, Sheffield Academic Press, Sheffield, 96–138 (2000).
13. T. Hirschfeld, 'Quantitative FT-IR: A Detailed Look at the Problems Involved', in "Fourier Transform Infrared Spectroscopy", eds J.R. Ferraro and L.J. Basile, Academic Press, New York, 193–242, Vol. II (1979).

Handbook of Vibrational Spectroscopy, Online © 2006 John Wiley & Sons, Ltd.

This article was published in the *Handbook of Vibrational Spectroscopy* in 2006 by John Wiley & Sons, Ltd.
DOI: 10.1002/9780470027325.s3101